January 2015

An Investigation Of Six Poorly Described Close Visual Double Stars Using Speckle Interferometry

Daniel B. Wallace

AN INVESTIGATION OF SIX POORLY DESCRIBED CLOSE VISUAL DOUBLE STARS
USING SPECKLE INTERFEROMETRY

by

Daniel B. Wallace
Bachelor of Science, East Stroudsburg University, 2008

A Thesis

Submitted to the Graduate Faculty

of the

University of North Dakota

in partial fulfillment of the requirements

for the degree of

Master of Science

Grand Forks, North Dakota
May
2015

This thesis, submitted by Daniel B. Wallace in partial fulfillment of the requirements for the Degree of Master of Science from the University of North Dakota, has been read by the Faculty Advisory Committee under whom the work has been done and is hereby approved.

_____
Dr. Paul S. Hardersen

_____
Dr. Russell M. Genet

_____
Dr. Kent Clark

This thesis is being submitted by the appointed advisory committee as having met all of the requirements of the School of Graduate Studies at the University of North Dakota and is hereby approved.

_____
Wayne Swisher
Dean of the School of Graduate Studies

_____
Date

PERMISSION

Title   An Investigation of Six Poorly Described Close Visual Double Stars Using Speckle Interferometry

Department   Space Studies

Degree   Master of Science

      In presenting this thesis in partial fulfillment of the requirements for a graduate degree from the University of North Dakota, I agree that the library of this University shall make it freely available for inspection. I further agree that permission for extensive copying for scholarly purposes may be granted by the professor who supervised my thesis work or, in his absence, by the Chairperson of the department or the dean of the School of Graduate Studies. It is understood that any copying or publication or other use of this thesis or part thereof for financial gain shall not be allowed without my written permission. It is also understood that due recognition shall be given to me and to the University of North Dakota in any scholarly use which may be made of any material in my thesis.

<div align="right">
Daniel B. Wallace
May 1, 2015
</div>

TABLE OF CONTENTS

LIST OF FIGURES

Figure | Page

LIST OF TABLES

ACKNOWLEDGMENTS

To my Mom and Dad, who have always encouraged me to learn and gain new perspectives through exploration, and to all my family and friends who have supported me during the course of this work.

ABSTRACT

Continued observation of double stars is necessary for confirmation of binarity and to provide updates to astrometric data used to compute accurate binary orbital parameters, thereby more accurately informing stellar mass estimations – the critical parameter from which stellar models are derived. In October of 2013, six double stars from the Washington Double Star (WDS) catalog exhibiting close separations, as well as significant deviations from previously published orbits, were observed and imaged using the speckle interferometric technique on the 2.1-meter telescope at Kitt Peak National Observatory (KPNO) in Arizona. The observations of the six double stars occurred as part of large, collaborative, eight-night, student-learning-centered observing run organized by principal investigator Genet of California Polytechnic Institute. The run produced in total roughly 1000 raw speckle images for each of the more than 1000 double stars and single reference stars observed, resulting in a total database of 1.4 terabytes. The speckle images for the targets, including the six targets investigated in this thesis, were taken using a relatively low-cost, portable speckle interferometry camera system developed by Genet, the heart of which is a lightweight, high speed, high signal to noise ratio (SNR) Andor electron multiplying CCD (EMCCD) camera capable of exposures on the order of tens of milliseconds. Exposures of 10-20 milliseconds are faster than atmospheric coherence timescales, and allow for the implementation of the speckle interferometry – the obtainment of diffraction-limited image information of binary stars defined by the full aperture of the telescope from the autocorrelation and Fourier analysis of randomly distributed, isoplanatically correlated speckle pairs, which represent the diffraction-limited images of the associated coherence cells above and

within the atmospheric area of the primary aperture (sub-apertures). Following the Oct. 2013 observing run, reduction and analysis of the speckle images for the six target binary stars (as well as five calibration binaries) and determination of the new astrometry was completed using the general purpose astrometry software program PlateSolve3 (PS3), written and developed by Rowe & Genet (2014).

Using the new astrometric data derived from the Oct. 2013 2.1-meter speckle observations, the previously published United States Naval Observatory (USNO) orbital plots for the six target doubles were updated to reflect the new, and in some cases missing measurements. Target double star orbits were reevaluated in light of the updates in order to draw conclusions about the characteristics of each proposed binary system. In all six target cases, continued trends in significant astrometric deviations from published orbits and ephemerides have been demonstrated by the new observations, indicating the need for orbital revisions of these binaries. Analysis of systems WDS22357+5413, WDS02231+7021, and WDS06256+2227 indicate rectilinear rather than Keplerian motion, and are concluded to likely be optical doubles. As a result of this work, two observations of WDS05153+4710 were shown to be erroneous and have been scheduled to be removed from this binary's WDS observational record (Mason, private communication, 2015).

Complementary to the central goal of investigating the six target close visual double stars via speckle interferometry, the entire effort demonstrated the applicability and utilization of relatively low-cost portable speckle camera systems on large telescopes, as well as the value and advantages of student participation and contribution within the realm of a large-scale observing run at a major observatory and the resulting peer reviewed scientific works that follow.

CHAPTER I
OVERVIEW

Introduction

From the Earth's perspective, one can survey a reasonably unpolluted night sky and observe many stars as close pairs, having separations much smaller than the diameter of the full moon. Many of these stars, termed double stars, are gravitationally bound, and more specifically referred to as binary stars. The two components of a binary star, the primary and secondary, orbit a common center of gravity and share a similar physical location in the galaxy. Other double stars are merely illusions called optical doubles. Optical doubles appear very near each other from the observer's perspective, but may actually be largely separated along the line of sight and are not considered to be gravitationally associated, apart from residing in the same galaxy.

Observational measurements of double stars, specifically the apparent position and separation of the two stars relative to one another, can be obtained using a variety of techniques such as visual micrometry, photometry, lucky imaging, and speckle interferometry. From these relative apparent position measurements, it is possible to obtain further information about the observed stars, such as the true orbital parameters, and in turn the masses of the components provided accurate parallax data is available (Argyle 2012). Coupled with accurate parallax data, binary star observations and orbit computations resulting from a record of visual astrometric measurements (or radial velocities determined from shifting spectral lines in the case of eclipsing spectroscopic pairs), remain the only current, reliable, and direct methods of stellar mass

determination (Massey & Meyer 2001). Accurate stellar mass estimates allow for better constraints of the empirical mass-luminosity (M-L) relationship (discovered by Hertzsprung and Russell in 1923), considered to be one of the fundamental descriptions of stellar properties, and the basis of modern developed stellar interior and evolution models, underscoring the great importance of accurate stellar mass determination through binary star observations (Heintz 1978, Couteau 1981, Massey & Meyer 2001, and Argyle 2012[2]).

Chapter 1 of this thesis will serve as an overview of double stars and double star science, including a review of the major milestones and developments related to the field over the past four decades, a discussion of the importance of double star science, and a theoretical description of the speckle interferometric technique which flows from the well-known interference phenomena of light. Chapter 2 describes the observations, including details of the 2.1-meter telescope, observational techniques, target selection, and specific data obtained during the October 2013 KPNO I speckle observing run. Chapter 3 reviews the methodology, including explanations of how the obtained data were reduced, analyzed, and interpreted, concluding with a discussion regarding the calibration, precision, and accuracy of the observations. The final chapter presents the findings, discussions, and conclusions regarding the work.

Statement of Problem and Experimental Hypothesis

The officially stated problem related to this thesis holds that many binary star systems remain unconfirmed, or are astrometrically poorly described. These problematic binaries, having prematurely published preliminary orbits of poor accuracy, necessitate the need for additional quality observations to help constrain the relative astrometry of the binary systems, leading to revised orbits and therefore improved stellar mass estimates. The experimental hypothesis of this current thesis states that one additional speckle interferometric observation of a poorly

described binary star system possessing a preliminary, low grade orbit, will contribute to the understanding of the system and provide further information necessary for the confirmation of binarity, or revision of the described preliminary orbit.

Double Stars

Observations and surveys of the night sky from the middle to late 20th century have shown that it is just as common, if not more so, for stars to exist in pairs or multiples, as it is for single stars to exist, as is the case with the Sun (Couteau 1981[2]). Mason & Hartkopf (2003) suggest that two thirds of the stars visible from our terrestrial perspective are binaries or multiples. Heintz (1978[2]) also offered disparity among multiple and single star systems, stating the observed area around the Sun shows clearly that single star systems are the minority. More specifically, Heintz (1978[2]) stated that 85% of observable stars are members of double or multiple systems, and held that some 20th century studies indicate 85% is likely a conservative estimate. The results of numerical studies by Jaschek & Gomez (1970), Abt & Levy (1976), and Duquennoy & Mayor (1991) indicate very high duplicity and multiplicity frequencies for stars within the galaxy. Argyle (2012[3]) agrees that multiple star systems are the rule, rather than the exception, in the solar neighborhood, and probably beyond. Such conclusions are quite logical if one considers that many stars are often born simultaneously and out of the same stellar nebula, in close proximity, according to current stellar formation and evolution models (Argyle 2012[4]).

However, more recent studies concerning the frequencies of single, double, or multiple star systems (hereafter referred to as multiplicity studies) have incorporated improved data constraints, such as those informing the initial stellar mass function (IMF) which indicates most stars in the galaxy are of spectral class M (relatively cool and low mass stars – red dwarfs). Recently, improved understanding of the relationship between multiplicity and spectral class has

suggested multiplicities very different than previously thought (Lada 2006). For example, surveys completed by Leinert et al. (1997), Reid & Gizis (1997), Delfosse et al. (2004), and Siegler et al. (2005) have indicated that binary frequency declines sharply from the G class value, being only around 30% for M class stars, and even lower for L and T class dwarfs – objects near or below the hydrogen burning limit of <.08 solar masses ($M_\odot$) (Gizis et al. 2003; Massey & Meyer 2001). Raghavan et al. (2010) conducted a survey of 454 solar-type stars via long-baseline interferometry and speckle interferometry, among other techniques, at the Center for High Angular Resolution Astronomy Array (CHARA), and concluded that the majority (54% ± 2%) of solar-type stars are single, in contrast to the results of prior multiplicity studies which suggested much lower percentages for unassociated solar-type stars. These recent efforts imply that if the galactic stellar population is primarily composed of M class stars, and that the multiplicity of M class stars, as well as G class stars, is comparatively low, then previously accepted ideas about the frequency of double and multiple star systems in the galaxy and beyond may be grossly overestimated, and that single stars are actually the majority (Lada 2006).

Regardless of the possible erroneous estimates of multiplicity made in the past, the galaxy undoubtedly still contains many double and multiple star systems that remain to be discovered, confirmed, and studied. Iconic examples of confirmed star systems which demonstrate multiplicity include systems such as the Trapezium within M42 (Orion) and the complex system of Alpha Geminorum (Gemini) as shown in Fig. 1. Although no binary star system has been observed in the act of formation, it is thought that binary stars typically come about when two stars are born in close proximity and become gravitationally bound about a common center of gravity, each star revolving around the Barycenter as a system under the influence of centripetal force due to the force of gravity, i.e. Keplerian motion (Argyle 2012[5]).

The specific mechanics of binary star formation are still not completely understood, but most experts agree that formation involves stages of early fragmentation resulting in condensing cores that become the components of the binary, followed by evolution via accretion and migration, thereby fixing the final masses of the components and the orbital parameters of the system (Halbwachs et al. 2003).
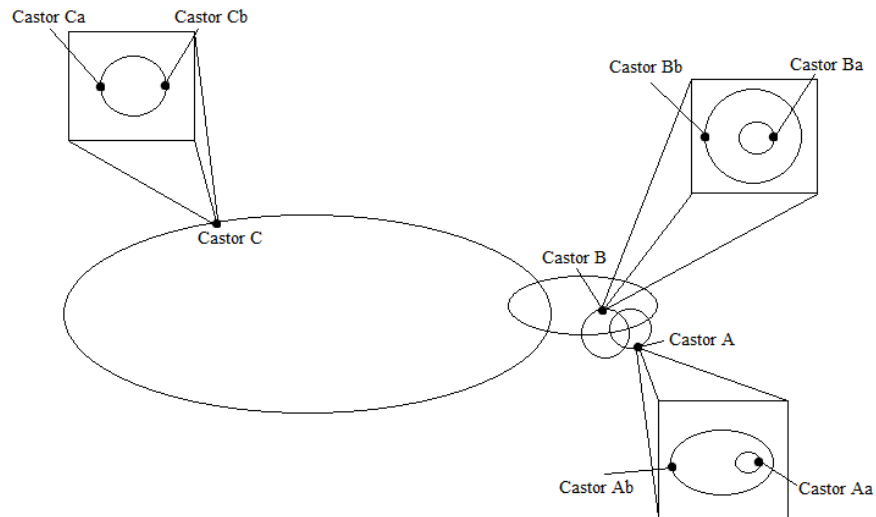
Fig. 1 – α Geminorum – the Castor sextuplet system. The estimated orbit of the Castor C and Castor AB system is greater than 10,000 years. The orbit of the smaller Castor B and Castor A system has been estimated to 476 years (Heintz 1988). Figure adopted from an infographic created by NASA's Jet Propulsion Laboratory.
http://www.jpl.nasa.gov/infographics/infographic.view.php?id=10884.

As previously stated, gravitationally bound double star systems are more specifically referred to as binary stars (Heintz 1978[3]). This distinction exists currently as the term *double star* has become a more general term referring to binary stars and also to optical doubles. Optical doubles, although relatively few in number compared to binary stars according to Couteau (1981[3]), are chance orientations, more accurately understood by applying the expression of two ships passing in the night (whether Couteau's conclusion regarding the frequencies of binaries vs. optical couples is correct remains to be seen). One star in an optical double may be

located light years away from its partner along the Z-axis, or line of sight relative to the observer, and thus the stars are not gravitationally bound about a common center.

Binary pairs which are truly gravitationally bound, however, may have such small physical separations that the surfaces of the components nearly touch – so called contact systems (Argyle 2012[6]). Normally, binaries so closely separated cannot be distinguished visually using normal ground-based telescopes and necessitate the application of advanced techniques to distinguish the stars, including spectroscopy (based on radial velocities and movement of observed spectral lines), astrometry (based on cyclical proper motion changes of a star compared to faint background stars due to the presence of an unseen orbiting companion), and photometry (based on eclipsing binaries and changes to measured light curves – see Fig. 2) (Argyle 2012[7]).
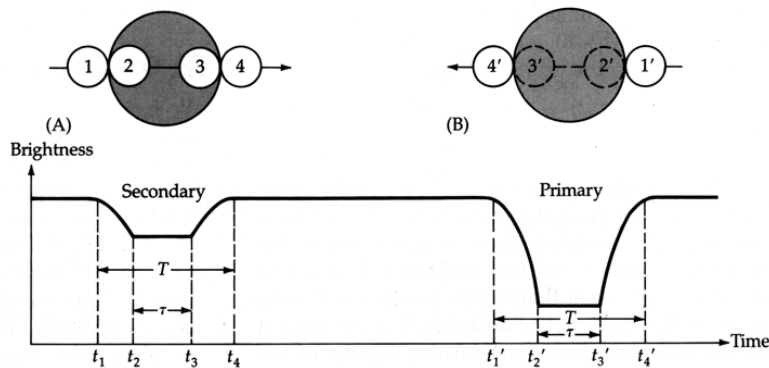
Fig. 2 – Diagram representing differential photometry typical of eclipsing binary systems. The system luminosity decreases slightly as the secondary eclipses a portion of the primary (A) and drastically as the primary completely eclipses the secondary (B). Eclipsing binary systems are only seen as such when the orbit appears at least slightly edge on as viewed by the observer. Source: http://ircamera.as.arizona.edu/astr_250/Lectures/Lecture_15.htm.

Thus, the major classes of binary stars (visual, spectroscopic, photometric, and astrometric) are derived from the various detection methods that exist – see Fig. 3. Recently developed advanced amplitude optical interferometry arrays such as CHARA on Mt. Wilson, which employs six 1-meter optical telescopes in a Y-configuration interferometer, can provide milliarcsecond (mas) resolution, allowing close binaries with orbital periods of just one day to be

resolved (McAlister 1999). More on the developmental history of binary star observing

techniques and current capabilities will be provided later in this chapter. Many double stars have

larger separations, allowing the observer to distinguish the components using simple

instrumentation such as binoculars or small telescopes, and are aptly named visual double stars.

There are even a few double stars that can be distinguished using the naked eye, such as Alcor

and Mizar (Ursa Major), and the more challenging $\epsilon^{1,2}$ Lyrae (Lyra), nicknamed the Double-

Double. The majority of naked eye doubles, however, are only optical doubles (King 2014).

This thesis deals exclusively with *close* visual double stars, best resolved and measured using

large aperture telescopes.
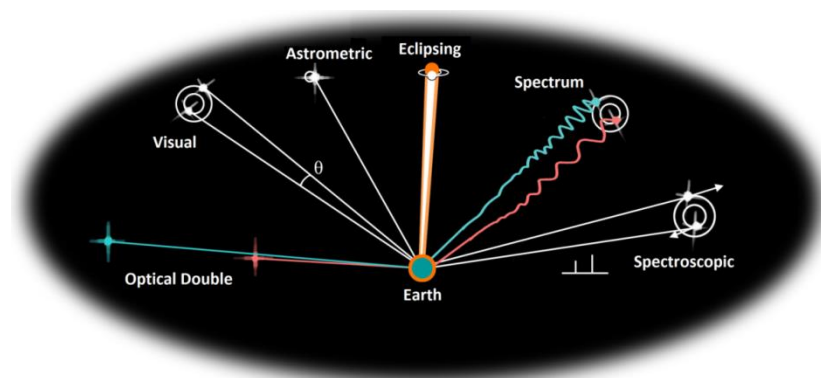
Fig. 3 – A simple schematic describing the major types of binary stars and their characteristics as seen from Earth. Schematic credit: https://quantumredpill.wordpress.com/2013/02/14/binary-stars/.

History of Double Star Science

Astrometric observations and measurements of double stars, consisting of position angle

(θ) measured in degrees (°), angular separation (ρ) measured in arcseconds (″), and epoch or date

of the observation (in fractional Besselian years) (see Fig. 4 for definitions), have been

meticulously kept by double star observers over the last two centuries. Published observations

and measurements have also been assembled into many catalogs over the same span of time,

mainly by the observers themselves – the first by Mayer in 1781 containing just 80 entries

(Heintz 1978[4]). The most up to date and widely accessed catalog is currently the United States

Naval Observatory's (USNO) Washington Double Star (WDS) catalog.
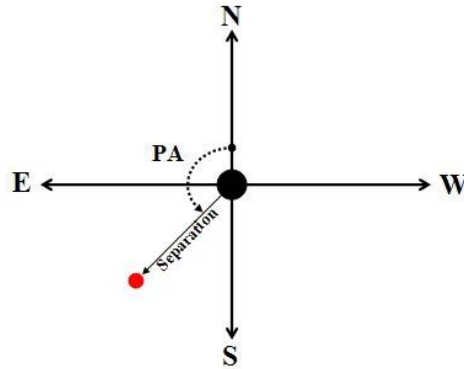
Fig. 4 – The principle double star position measurements: Position Angle (PA or *θ*) is the angle between celestial north (representing 0° and 360°) and the line joining the components, represented here by the dotted line, in this case 135°; Angular Separation (*ρ*) is the apparent separation of or distance between the components measured in arcseconds or fractions thereof. The large black center circle is the primary star taken as the origin, and the red circle is the secondary star. Credit: Breit (2007). Source: http://www.poyntsource.com/Richard/double_stars_video.htm.

According to the WDS, over 120,000 double stars have been identified as of 2015. Of

these systems, 18,624 are confirmed physical binaries, 4,293 are optical couples, and 106,389

remain unconfirmed (USNO 2015a). Since its inception and official adoption as the double star

field's principal catalog in 1964, the WDS has grown considerably as observing techniques

mature, diversify, and produce higher quality data (see Fig. 5). Several generations of
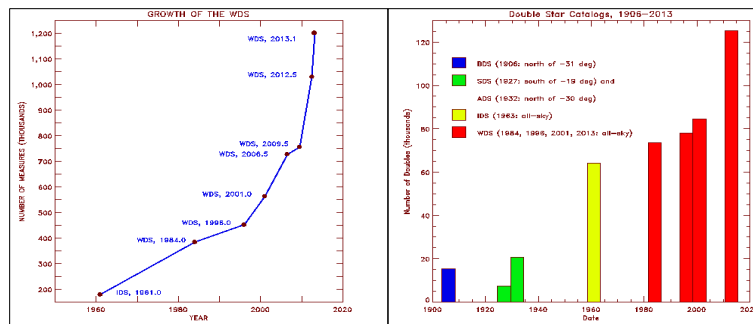
36. Fig. 5: Growth of Washington Double Star catalog & comparison of major double star Catalogs of the 20ᵗʰcentury. (left) Growth in the number of measures in the Washington Double Star catalog since its inception in the early 1960's. The 1984.0, 1996.0, 2001.0, and 2006.5 editions of the WDS are indicated as well as more recent dates. (right) Comparison of major double star catalogs of the 20ᵗʰ century. Credit: USNO. Source: http://ad.usno.navy.mil/wds/wdstext.html#unpublished.

astronomers keeping detailed records of their observations and measurements of double stars were necessary to arrive at such a catalog, as well as the current catalog of published binary star orbits – the USNO's 6th Orbital Catalog containing 2,518 orbits of 2,413 systems (as of September 2014). It can be seen then, that the history of this specific astronomical field is vital, and although not the focus of this thesis, a brief historical review of double star science is warranted.

Double star science offers a relatively short history, spanning slightly more than two hundred years, compared to the long history of astronomy in general, which likely began with mankind's first pensive views of the heavens tens or perhaps even hundreds of thousands of years ago. Much of the historical literature on the subject of double stars considers the observations of William Herschel in the late 18th century to be the formal inception of double star astronomy (Couteau 1981[4]). However, more detailed historical records reveal observations of celestial objects, akin to what would be considered today a double star, dating back to the observations of Claudius Ptolemy in the 2nd Century AD (Heintz 1978[5]). Considering the significance placed on celestial observation in the ancient world, it is reasonable to conclude that ancient observers, prior even to the celestial minded Ancient Greeks, Egyptians, and Babylonians, would have noted certain pairings observable to the naked eye, such as the pair of Alcor and Mizar in today's Ursa Major.

The history of double star astronomy reveals a steady increase of formally published works related to the field from year to year beginning with Herschel's first published works in the late 18th and early 19th centuries. The history also suggests an overall rapid evolution of observational and analytical techniques beginning with visual observations through small 17th century telescopes by observers such as Riccioli, and the first thoughts of gravitationally bound

stars beyond the Sun occurring to Lambert as early as 1767 (Heintz 1978[6]). Since binary star

observation allows for one of the only direct avenues through which the understanding of stellar

physical parameters, other than those of the Sun, can be ascertained and refined, one can easily

see how the evolution of double star science has significantly influenced the understanding of

stars in general.

Technological advancement, as with most sciences, has greatly enhanced our ability to

observe and analyze double stars. For example, the development of larger aperture telescopes,

up to those of 3-10 meters, and optical interferometic arrays forming effective apertures of tens

to hundreds of meters, has allowed for greater detection and resolution ability of faint light

sources. Charged couple device (CCD) and EMCCD (electron multiplying) cameras have all but

replaced traditional film and photographic plate imaging in professional work, enabling much

faster, more sensitive, more accurate and less subjective (compared to visual observations)

imaging of celestial objects at a fraction of the labor and necessary material, and equipment

resources. CCD camera imaging also provides a permanent record of the observation, to which

other astrometrists can refer as long as the image exists. The application of speckle

interferometry, devised by Labeyrie (1970), can enable the extraction of diffraction-limited

image information, allowing for much more detailed resolution using large ground-based optical

telescopes than would otherwise be possible. Speckle interferometry, the technique at the heart

of this current work, is applied in order to circumvent atmospheric distortion of incoming

starlight, commonly referred to as seeing limitations, and allow for the obtainment of diffraction-

limited information of celestial targets with small angular size such as close double stars

(Labeyrie 1970; Hoffmann 2000). Today, the tools and techniques of double star observation

vary widely depending on the type and difficulty of the pair to be observed, as well as the resources of the observer.

Typically, closely separated double stars are very challenging to resolve, and can only be done so using expensive non-visual spectroscopic, photometric, or astrometric techniques. Thus, inherent to double star science is a so called resolution gap, which represents the gap between the resolution limits of various visual and nonvisual observation techniques.

However, recent advances in speckle interferometry, namely the application of the technique on very large aperture telescopes with advanced adaptive optics systems such as that of the 3.5-meter telescope at the WIYN observatory at KPNO, as well as the application of long-baseline optical interferometry like that of the Cambridge Optical Aperture Synthesis Telescope (COAST – Cambridge, UK), the Navy Optical Interferometer (NPI – Anderson Mesa, Arizona), and the CHARA array (Mt. Wilson, Southern California) have enabled closure of the resolution gap (McAlister 1988). Indeed, resolutions of binaries only previously detectable using expensive and complex ground-based spectroscopic techniques, or space-based telescopic observation methods have been achieved using relatively inexpensive techniques like speckle interferometry, albeit on relatively large telescopes (Mason & Hartkopf 2003). Optical interferometer arrays like COAST, NPI, CHARA, and the Sydney University Stellar Interferometer (SUSI – near Narrabri, New South Wales) have enabled visual resolutions on the order of milliarcseconds, and future interferometic array projects such as the Magdalena Ridge Optical Interferometer (MROI – currently under construction, South Baldy Ridge, New Mexico) will yield angular resolutions below 1 mas (Argyle 2012[8]).

Significance of Double Star Science

An enormous influx of double star observations and associated data has resulted from recent space-based astrometry missions such as the European Space Agency's (ESA) Hipparcos mission (1989-93) and current missions such as ESA's Global Astrometric Interferometer for Astrophysics (GAIA) mission (2013-2018). Quality follow-up work including further observation and analysis of targets is needed (Perryman 2012). However, close visual double star observing programs involving large telescopes which are powerful enough to resolve many of the close visual double stars observed during space-based astrometry missions are not very common, leaving large numbers of recently discovered double stars underobserved, unconfirmed, or otherwise neglected (Mason & Hartkopf 2003). To be sure, the USNO currently maintains a sizeable list of so called neglected doubles, and one can observe that this list contains nearly forty thousand separate objects (USNO 2015b). Visual observations of close double stars from ground-based observatories necessitate large aperture telescopes (Genet 2013a), which, like the close visual double star observing programs, are relatively few in number compared to the number of important astronomical research initiatives that compete each year for time on such large telescopes. Many large-scale national observatories which maintain and operate large, expensive telescopes, such as KPNO, are federally subsidized, and are inclined to accept project proposals which correspond to Federal mandates, thus attracting Federal financial support (Genet, private communication, 2014). Considering this, Genet (2013a, 2012b) offers that student-learning-centered double star observing runs at major observatories around the world organized and guided by experts in the field of double star science, and employing low-cost portable speckle camera systems, can help address and alleviate the plight of today's data-burdened professional double star astronomers. Such student-learning-centered observing runs at

major observatories with large telescopes would, at the same, time address national directives regarding science, technology, engineering, and math (STEM) education by providing invaluable learning experiences for students interested in the field of double star science and astronomy.

Student-centered double star observing runs, such as that described in this thesis, provide a threefold solution to the aforementioned double star neglect issues: (1) under the instruction and guidance of professionals, students participating in observing runs at major observatories with large telescopes can learn and gain significant hands-on experience in a specialized area of astronomy, while (2) making valuable and much needed contributions to the field of double star astronomy, addressing the inherent lack of follow-up work. Lastly, (3) student-centered programs address the need for the development of the next generation of astronomers who will work with the multitude of data being acquired through advanced technologies – a need expressed in recent decadal recommendations by the National Academy of Science and National Research Council (Henry et al. 2009).

Aside from providing crucial hands-on instruction to the next generation of astronomers, double star science continues to be vital to the development of stellar formation and evolution models. Observation and mathematical analysis of binary systems allows for the determination of physical properties of stars, in particular stellar mass (Argyle 2012_9). Information about stellar masses, which can only be directly derived from computed binary star orbit parameters based on a record of astrometric measurements (or spectroscopic information), and accurate parallax data along with laws of Newton and Kepler (inferences of stellar mass can be made indirectly using stellar models), allows for testing and refinement of stellar models (discussed below), and in a larger context, influences current cosmological understanding in general (Argyle 2012_{10}; Genet 2013a). Couteau (1981_5) offers that, in the context of stellar mass determination,

13

orbital solutions from binary star measurements, along with accurate parallax and distance information, are the primary goal of double star astronomy.

Conclusions by Mason & Hartkopf (2003) regarding stellar mass estimations also suggest that binary star measurements via speckle interferometry can provide: independent checks on proper motions of close double stars, verification or confirmation of close visual binaries found by other techniques (e.g. Hipparcos and Gaia), and information as to the multiplicity characteristics of a large sample of stars. Mason & Hartkopf go on to further advocate for speckle interferometric investigations of double stars, proposing that such work can aid in the study of stars in planetary searches by removing from targeted searches stars unlikely to have life harboring planets, or ensuring spectroscopically detected exoplanets are not pole-on binary stars (Mason & Hartkopf 2003).

Binary Stars and Stellar Mass Determinations

Plotting a series of several binary star astrometric measurements (θ and ρ, see Fig. 4) against time for a true binary star would produce a curve indicating Keplerian motion (assuming a relatively short period binary or data series spanning a large amount of time). Given a data series spanning the entire orbital period of a binary star, the observed curve would reveal an ellipse known as the apparent orbit of the binary (see Fig. 6). This curve is the apparent path of the secondary star, which is often the fainter component, around the center affixed primary star (the primary and secondary actually orbit a common center of gravity, but to simplicity's sake the primary is represented as fixed, leaving just the orbiting secondary) (Argyle 2012[11]). The apparent orbit is the projection of the true orbit onto the celestial sphere relative to the observer's point of view.
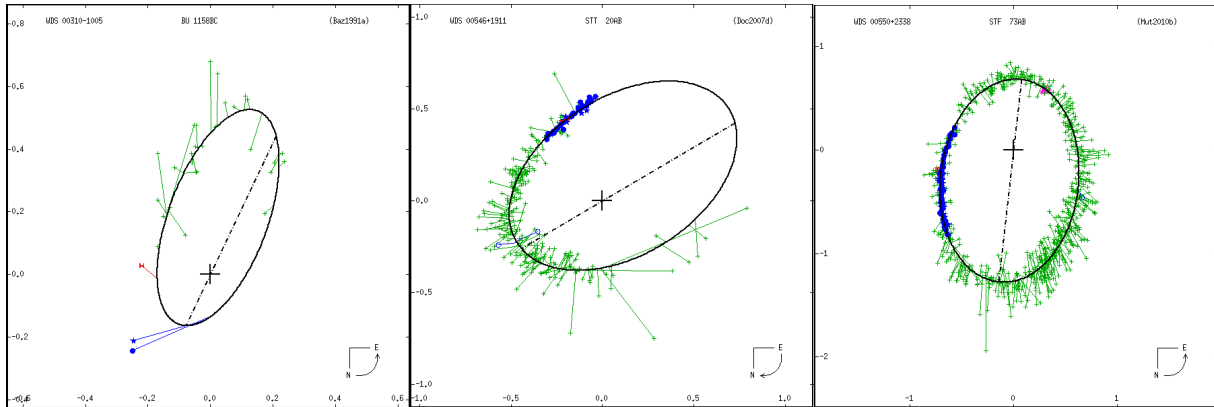
Fig. 6 – Examples of USNO Orbital Plots. (Left) USNO orbital plot of WDS00310-1005, (Center) plot of WDS00546+1911 & (Right) plot of WDS00550+2338. In all plots, visual (usually micrometric) observations are shown as a green +, photometric as purple *, while speckle observations are shown as the blue • (USNO Speckle = blue star). Red H and T reflect Hipparcos and Tycho measurements respectively. Lines connecting measurements to computed orbit (bold black ellipse) reflect observed minus calculated (O-C), based on computed ephemerides, for θ and ρ, for the respective epoch. The large black plus sign represents the location of the primary star. Celestial north and orbital motion is indicated by the figure in the lower right. Scales are in arcseconds. The left and center orbital plots demonstrate a record of astrometric measurements which cover only a fraction of the complete orbit, while the plot on the right reflects complete orbital coverage with no observational gaps. The left orbital plot is characteristic of poorly described binary systems, as deviation from computed orbit in this case can clearly be seen from the recent Hipparcos and speckle observations; while the other two plots represent well defined systems and orbits which would receive high orbital grades based on USNO standards. (USNO 2015d).

With the apparent orbit known, elements of the true orbit can be ascertained. According to Heintz (1978[7]) the four descriptive elements for the true orbit are:

P – the orbital period in years; alternatively the mean motion per year ($n = 36/P$ or $\mu = 2\pi/P$) is given

T – the epoch of passage through periastron (the minimum separation between components) in Besselian years and fractions thereof

a – semi-major axis of the true orbit in arcseconds

e – the numerical eccentricity.

Three additional descriptive elements determine the projection of the true orbit into the apparent orbit, and depend on the orientation of the orbit to the observer:

Ω – the position angle of the ascending node or the position angle of the line of

intersection between the tangential plane of projection and the true orbital plane, there are two nodes differing by 180° which can only be determined from radial velocity data

i – inclination, the angle between the plane of projection and that of the true orbit, which ranges from 0°-180°

ω – the argument of periastron or periapsis – the angle in the true orbit plane from the node as given under Ω to the periastron, reckoned in the direction of motion, ranging from 0° to 360°.

Computation of both apparent and true orbital elements, a topic beyond the scope of this current thesis, involves complex geometric and/or analytic methods. Presently there is no one method that can handle all the various types of observed binary star configurations (Argyle 2012[12]). Classical geometric methods, the method of Thiele, Innes, and van den Bos, and iterative analytic methods such as the method of Danjon and Rabe, are typically used for orbital element computation or revision (Heintz 1978; Couteau 1981). More recently developed methods include that of Hartkopf et al. (1989), which describes a grid search method of orbital calculation and orbital revision.

Orbital solutions, combined with information regarding the binary star's distance from our solar system ascertained through accurate parallax measurements, allow for an estimate of dynamical stellar mass sum to be made by way of Kepler's third law. For example, Newton's version of Kepler's 3rd law, formulated for the total mass of a binary star system, can be used as follows:

$$m_1 + m_2 = \frac{a^3}{(\pi^3)P^2}$$

In the above equation, m_1 and m_2 are the masses of the components in units of solar mass ($M_\odot$), a is the apparent semi-major axis (arcseconds), π is the absolute trigonometric parallax (arcseconds), and P is the period of the system (years). From the equation, one can see that total

mass of a binary system is directly proportional to the cube of the semi-major axis, and inversely proportional to period squared, with both semi-major axis and period being derived from the true orbit solution. Thus, a small change in the semi-major axis and period resulting from revised orbits, perhaps due to new and more accurate astrometric measurements, will result in a large change in the computed total system mass, rendering accurate astrometric position measurements and the orbits they inform critical. Accurate parallax measurements have traditionally been the most limiting factor for accurate stellar mass estimations, but recent parallax measurements from the Hipparcos mission and GAIA mission have and will provide parallax data an order of magnitude more accurate for more than tens of thousands of binary stars (Genet 2013a; Massey & Meyer 2001). This will provide many opportunities for stellar mass estimation revision.

As mentioned earlier, stellar mass is the key component to our development of stellar models which are validated through testing against the empirical mass-luminosity relationship (MLR), discovered and described by Hertzsprung and Russell in 1923, and soon after theoretically demonstrated by the work of Eddington. The MLR revolutionized mankind's understanding of the stars in the universe, providing objections to previously established notions such as that stars evolved from giants to dwarfs (Heintz 1978[8]). Eddington's approximation of the relationship between the measure of the total radiation of a star (the luminosity or *L*) and the mass of the star (*M*), $L \sim M^4$, was at first widely accepted, but as range of stellar mass became better defined, it became clear no single exponent would describe the dependence of luminosity on mass. Presently, Massey & Meyer (2001) describe the following approximations of the mass-luminosity relation for various stellar mass ranges:

$$L \sim M^{1.6} \, (M \approx 100 M_{\odot})$$

$$L \sim M^{3.1} \, (M \approx 10 M_{\odot})$$

$$L \sim M^{4.7} \ (M \approx 1M_\odot)$$

$$L \sim M^{2.7} \ (M \approx 0.1M_\odot).$$

Massey & Meyer (2001) also cite that other stellar properties are derived from the MLR, for example, main-sequence stellar lifetimes (τ_{MS}) are roughly proportional to the mass (amount of fuel) and inversely proportional to luminosity (how quickly the fuel is consumed), i.e. $\tau_{ms} \sim M/L$. Given the aforementioned M-L relations, more specific estimates for stellar lifetimes can be determined, such as $\tau_{MS} \sim M^{-3.7}$ for solar-type stars. Well defined estimates for stellar masses, and thus other stellar properties, are given for most stars across the known stellar mass range of $0.08 - 150M_\odot$, however it is still unclear what, if anything, limits how massive a star can be. Low mass stars have a clear temperature limitation required to burn hydrogen or deuterium in the stellar core, allowing for stars down to $0.015M_\odot$ (Massey & Meyer 2001).

To further highlight the importance of accurate stellar mass determinations via observation and measurement of binary stars, one can consider how stellar models derived from the MLR are in turn used to indirectly approximate stellar mass, and it is through such means that the masses of most of the stars used to determine the initial mass function (IMF) are inferred (Massey & Meyer 2001). The IMF is the distribution of stellar masses upon formation from clouds of gas and dust in space, and can give information regarding the number of stars representing the different mass ranges in the galaxy as well as clues to the processes of stellar formation. According to the Russell-Vogt theorem, determination of stellar structure and evolutionary properties including luminosity, radius, temperature, density and the variance of these parameters as a function of time can occur only through knowledge of a star's mass and chemical composition (Kahler 1978). However, the range of possible stellar mass is much

greater than the range of chemical composition, thus it is a star's mass at birth which is the

principal determinant of its structure and evolution (Massey & Meyer 2001).

The binary star parameters θ and ρ, which inform stellar mass determinations as

described above, can be measured using several techniques including (from oldest to most

recently developed): visual micrometry, interferometry, speckle interferometry, lucky imaging,

lunar occultation, long-baseline optical interferometry, and space-based astrometry. The

following section will discuss the details of speckle interferometry, the technique applied in the

current work.

History of Speckle Interferometry

Speckle interferometry, first devised by Labeyrie (1970), has been the principle method

of binary star measurements for the past four decades, and is the modern offspring of a much

older technique used for stellar observation and resolution known simply as interferometry.

Interferometry, stemming from Young's double slit experiment in 1803 and the

Michelson-Morley experiment in 1887, was first used to measure widely separated double stars

by Schwarzschild in 1895, shortly after Michelson himself used the technique to measure the

angular diameters of the Galilean moons in 1891, and later the diameters of a handful of nearby

bright stars in 1919 (Michelson 1891; Mason and Hartkopf 2003). Today, interferometry and

various related techniques such as speckle interferometry, intensity interferometry, heterodyne

interferometry, and the recently established (within the past decade and a half) long-baseline

optical interferometry, are some of the most advanced techniques applied to binary star

measurement besides those involving space-based telescopes. Many developments have been

made in the field since Schwarzschild first applied the interferometric technique, and after more

than a century of progress, diffraction-limited resolution (that is, resolution limited by the

telescope employed rather than atmospheric distortion limitations) and image information is now commonplace. As mentioned previously, resolutions down to 1 mas have been achieved using optical interferometry with widely spaced telescopes (long-baseline optical interferometry) (Monnier 2003).

Beginning with speckle interferometric observations made by Gezari, Labeyrie, & Stachnik (1972), Labeyrie et al. (1974), Beddoes et al. (1976), McAlister (1977), and Blazit et al. (1977), tens of thousands of speckle measurements have been made, and scores of new binary stars have been found or confirmed using the technique. For example, McAlister (1988), the director and founder of Georgia State University's Center for High Angular Resolution Astronomy (1985-present) and former director and chief executive officer of the Mount Wilson Observatory (2003-2013), along with colleagues, had by 1988 made over 6,000 measurements of nearly 1,200 binary stars via speckle interferometry using the 4-meter Mayall telescope at KPNO, representing at the time more than 85% of all speckle measurements. Interestingly, the Hubble Space Telescope (HST) mission may well have been saved from a fate of uselessly observing hundreds of unsuitable guide stars found to be binaries through an emergency speckle interferometric investigation by McAlister. The HST guide star list investigation was initiated by the work of Shara et al. (1987), formerly of the Space Telescope Science Institute, who accurately predicted an estimation error in binary star frequency among the HST's selected guide stars. Binary star observations and measurements made using speckle interferometry have been compared against data obtained using classical techniques, and it is clear that speckle interferometry can produce highly accurate binary star data, being in fact more accurate and precise by an order of magnitude than classical visual measurements, providing confidence for the measurements of close binary stars the speckle interferometric technique is most commonly

applied to (McAlister 1977). Recent speckle interferometry applications include follow up of

Hipparcos, Tycho, and GAIA observations obtained thus far, determination of globular cluster

proper motion, extrasolar planet detection, and determination of asteroid duplicity detection

limits (Mason and Hartkopf 2003).

The Interference Phenomena of Light

Speckle interferometry, like basic interferometry, flows from the principle of linear

superposition, which describes the interference phenomena associated with light, including

constructive and destructive interference, and Fraunhofer diffraction of plane-wave light. These

characteristics of light, regarding astronomy and specifically double star science, pose natural

limits on resolution (see diffraction limit and Rayleigh criterion below), but also allow for

imaging methods which circumvent atmospheric turbulence or seeing limitations which normally

plague all ground-based optical telescope observations (see speckle interferometry below).
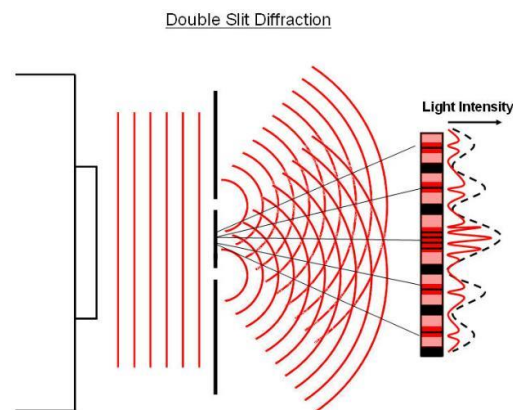
Fig. 7 – Interference Phenomenon: When coherent, parallel plane wave (e.g. laser at particular wavelength) light passes through two very narrow, and very narrowly spaced slits, the result is two wave patterns that overlap and interfere both constructively and destructively, producing a series of bright and dark fringes on a detection screen downrange of the slits. Credit: www.cronodon.com, BotRejectsInc (2015).

When coherent electromagnetic wave fronts, or plane wave light like that of a laser or

star, pass through a given point such as a thin slit defined on either side by opaque barriers, or

two slits as in Young's famous double-slit experiment, the secondary wavelet wave fronts

emanating from each of the infinite wave front points along the original wave front located at the

slit(s) (as described by the Huygens' principle), will diffract giving rise to distance differentials

between these wave fronts created past the barrier, and thus interference of these wave fronts. If

a screen is placed downrange of the slit(s) at distance D, the interference will be visible as an

interference pattern, or fringe pattern, made up of alternating bright and dark fringes, showing a

symmetrical intensity decrease outward from the central bright fringe in both directions (see Fig.

7 above).

Different wave fronts emitted by the Huygens sources at the slit(s) which travel the same

D to the screen, or those which maintain distance differentials (ΔD) corresponding to the source

light wavelengths (λ_0), or integer multiples thereof (i.e. $\Delta D = \lambda_0, 2\lambda_0, 3\lambda_0$, etc.) will arrive at the

screen in phase – peak-to-peak and trough-to-trough – interfering constructively, producing a

bright fringe. Conversely, wave fronts with distance differentials corresponding to odd integer

number of half wavelengths, or $\Delta D = 1/2\lambda_0, 3/2\lambda_0, 5/2\lambda_0$, etc., arrive at the screen 180° out of

phase – crest-to-trough, interfering destructively, effectively canceling one another and

producing dark fringes (Cutnell & Johnson 2004).

Analogous to the fringe pattern observed from the single or double slit demonstrations

described above, is the circularized Airy pattern formed when plane-wave light passes through a

circular aperture having a sharp edge, such as that of a telescope. The pattern, in the case of star

light seen at the focal plane of a refracting telescope for example, appears as a series of faint

concentric bright and dark circular fringes around a central star disk called the Airy disk (also

known in astronomy as the Point Spread Function or PSF), which is composed of ~84% of the

star light (see Fig. 8). The Airy pattern is the diffraction pattern created by the same
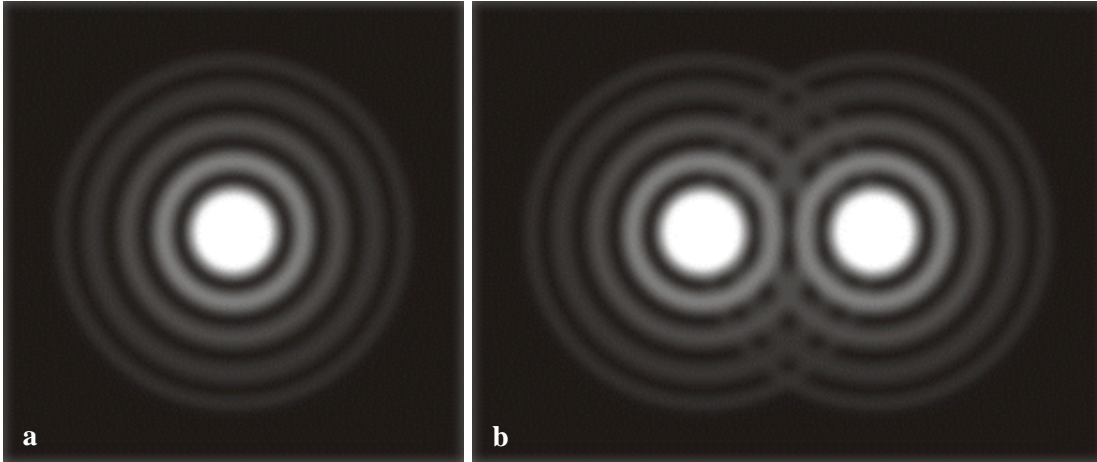
Fig. 8 – Airy Patterns: (a.) The Airy pattern consisting of bright central (maximum intensity) fringe and concentric dark and bright fringes. (b.) Two closely spaced Airy patterns still easily distinguishable but approaching the diffraction limit where the zeroth fringes would be difficult to distinguish. From Cutnell & Johnson, Physics 6th ed., 2004.

aforementioned interference phenomena, and creates the natural resolution limit for any optical instrument utilizing a circularized aperture to distinguish between two closely spaced objects. If two Airy patterns, for example of a double star, are sufficiently close, then the theoretical angular resolution limit (θ_{min}) in radians for the Airy disks is given by the Rayleigh criterion:

$$\theta_{min} = (1.22) \frac{\lambda}{D},$$

where λ is the wavelength of the light in centimeters, and D is the diameter of the aperture in centimeters. θ_{min} can be converted to arcseconds, the unit more commonly used to expressed angular resolution limits in astronomy, by multiplying by 206,265 arcseconds/radian).

The Airy pattern is rarely seen in large ground-based optical telescopes due to the destruction of the image from atmospheric turbulence (more on this subject below). Atmospheric turbulence, or seeing, imposes angular separation limits on telescopes that are orders of magnitude greater than theoretical resolution limits given by the Rayleigh criterion or by Dawes limit (not discussed here – see Argyle 2012, chapter 10). For example, a 4-meter telescope should be able to resolve an angular separation down to approximately 0.025

arcseconds; however in practice that same telescope could only hope to resolve separations of 1-3 arcseconds due to seeing limitations (Dainty 1981).

The seeing limitations imposed by the atmosphere are problematic if one wishes to resolve fine detail like stellar diameters or closely separated binary stars using ground-based telescopes of large aperture. Fortunately, through the development of interferometers, speckle interferometry, and related techniques such as lucky imaging, seeing limitations have been successfully surpassed.

Using Interference Phenomena for High Angular Resolution

The interference and diffraction phenomena associated with light can be employed in the field of double stars and other astronomical work that involves angular resolution of very distant celestial objects. For example, one can imagine the first stereoscopic interferometer built and installed by Michelson & Pease in 1919 on the 100 inch Hooker telescope at the Mt. Wilson Observatory, in which two flat mirrors spaced twenty feet apart on a beam were used to collect light from a star. The starlight was then directed into the telescope via a second pair of flat mirrors, and interfered at the focal plane, to form a fringe pattern (see Fig. 9).
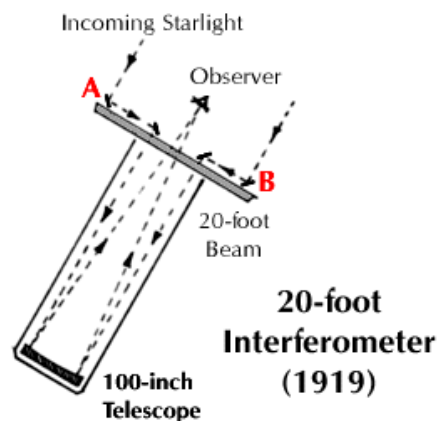
Fig. 9 – Schematic of the MWO Hooker telescope interferometer with two collecting mirrors A and B spaced 20ft. apart to form the interferometer. Source http://www.mtwilson.edu/vir/100/20fti/index.html Credit: www.mtwilson.edu (2015).

Armed with the knowledge of the distance between the fringes, the distance between interferometer and fringe pattern, the distance to the light source, and the wavelength, Michelson & Pease successfully determined the diameters of six close, bright stars using the Hooker telescope interferometer.

Designs of interferometers progressed in the first half of the 20th century to use more manageable screen slits, like that used in Young's double slit experiment (see Fig. 7), embedded within the telescope at the focus, or even between observer and eyepiece as Finsen (1964) had developed and used near the middle of the 20th century. Regardless of design however, early interferometric applications of the 20th century were disadvantaged because the full aperture of the telescope could not be used owing to the employed slit screen or aperture mask, and because the long baselines needed to resolve close binaries were difficult to engineer. Therefore the technique was limited to fairly bright objects, such as the brightest stars and the Galilean moons of Jupiter (Heintz 1978[9]).

Speckle Interferometry & the Speckle Pattern
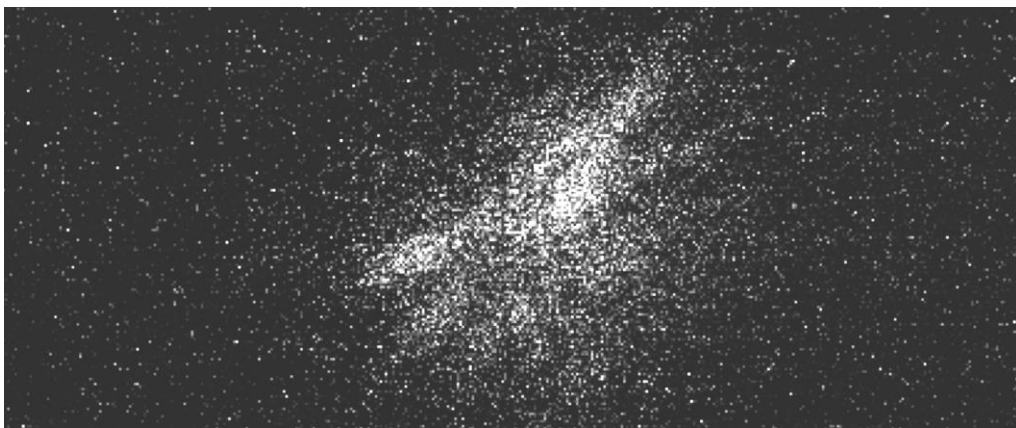
Fig. 10 – A single speckle image (WDS00101+3825) exposure typical of a 10-60 millisecond exposure using the Andor Luca-R EMCCD camera installed on the 2.1-meter telescope at KPNO during the Oct. 2013 observing run (see chapter 2 for a description of the observations).

Like classical interferometry, speckle interferometry also takes advantage of the interference and diffraction phenomena of light to resolve distant, closely spaced celestial

objects, whose light is essentially coherent; but unlike the early interferometric methods of Schwarzschild & Michelson, speckle interferometry uses the full aperture of the telescope to observe the image of a star or double star, which in one instant at the focus of a large telescope (>.3m) appears as a random conglomeration of specks (hence the first term of speckle) – see Fig. 10 (Labeyrie 1970; Dainty 1981).

Using a sufficiently powerful eyepiece, a dynamic speckle image, similar to the static speckle image shown in Fig. 10, can be seen visually by an observer, albeit with considerable difficulty, which Couteau (1981[6]) likened to a bunch of grapes. The static speckle frame above is a product of atmospheric turbulence frozen over a very short time period, such as those of millisecond electronic imaging exposures. To fully understand this image and the process of speckle interferometry, one must first recognize that within the column of air immediately above the primary telescope aperture in the direction of the target, there are many pockets of dynamic atmospheric cells, called isoplanatic patches or coherence cells, characterized generally by their average diameter (r_0 – "the Fried parameter") and duration (τ_0) (Argyle 2012[14]).

These dynamic atmospheric cells, with r_0 values on the order of 10 cm and τ_0 of ~15 milliseconds (ms), are the principle cause of telescopic image destruction (atmospheric seeing) over viewing times greater than the cells' average lifetimes ($> \tau_0$). Over short time scales, coherence cells appear, grow, disappear, and move about due to temperature and pressure gradients in the atmosphere, typically limiting angular resolution of telescopes to about 1 arcsecond (Hoffmann 2000). During the lifetime of the dynamic cell, the image as seen through a single cell of a close binary star (so close that the light from both components propagates through a single isoplanatic patch, i.e. $\rho < r_0$), is the diffraction-limited image of the binary

visible on the focal plane as a speckle pair (Argyle 2012[15]). The diffraction limit of the

coherence cells, or sub-apertures is defined by

$$\theta = 1.22(\lambda/r_0).$$

There can be hundreds or thousands of isoplanatic patches above the objective of a given

telescope $(D/r_0)^2$, and thus as many diffraction-limited speckle pairs, with differences

corresponding to cells of varying properties, which form the speckle frame of the binary – a

complicated interference pattern called a speckle pattern or interferogram (see Fig. 10)

(McAlister 1992). The random distribution of individual speckle pairs over the seeing disk

results from the refractive index differentials maintained over τ_0 of many coherence cells of

varying orientation, temperature (density), and size, thus producing constructive (and

destructive) interference of the diffraction-limited images (see Fig. 11).
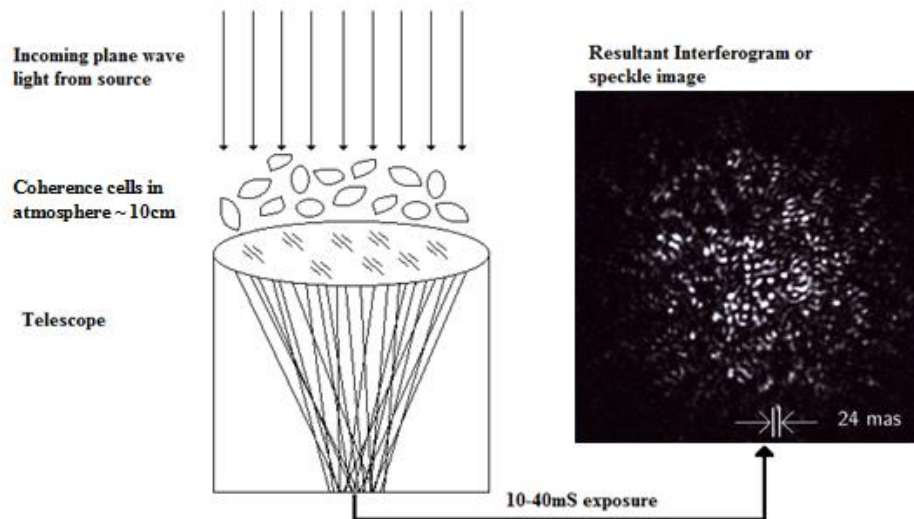
Fig. 11 – Interferogram, or speckle pattern formation schematic: incoming plane-wave light encounters coherence cells which attenuate the traversing light resulting in differential refraction. Corresponding coherence cells will produce constructive and destructive interference of the light, producing the speckled pattern. Short exposures ($<\tau_0$) freeze the image, preserving diffraction-limited information of the target. Scale in speckle image is typical of current work on large aperture telescopes.

Telescope aberrations can also contribute to the transformation of incoming starlight into

speckle patterns (Argyle 2012[15]). Moreover, the entire speckle pattern changes over short time

periods corresponding to τ_0; however, a very short exposure of less than 10-15 ms can essentially freeze the speckle pattern, preserving diffraction-limited, and thus high angular resolution information of the binary which can be extracted by assessing the frequency of spatial separations of the speckles via an autocorrelation function of the speckle frame or series thereof (Labeyrie 1970; Hoffmann 2012).

Extracting Diffraction-Limited Astrometry from Speckle Images

Although one speckle pattern frame may not appear particularly useful or even discernable, within the pattern there will exist a correlation among speckle pairs due to propagation of the close binary image through similar coherence cells, as described above. This correlation is called isoplanicity, and is the critical property that allows for the speckle spatial separation frequency assessment by the way of Fourier analysis of an individual speckle frame in order to extract full-aperture diffraction-limited image information of a close binary star observed using a large aperture telescope (as before close is defined as $\rho < r_0$) (Labeyrie 1970; Mason & Hartkopf 2003; Horch 2006).

As described by Mason & Hartkopf (2003) and Argyle (2012[14]), the essence of speckle interferometry is an assessment of the frequency of spatial separations and orientations of the speckles – each speckle from every other speckle, over the entire speckle frame. In the case of binary stars, the phrase speckle interferometry represents the attainment of astrometric measurements using diffraction-limited (or nearly so) images of binary stars, defined by the full aperture of the telescope employed, from the Fourier analysis of isoplanatically correlated speckle pairs. These speckle pairs represent the diffraction-limited images of the associated coherence cell sub-apertures within the atmospheric area above the primary aperture. Due to the inconsistency of refraction between coherence cells, binary speckle frames will have many

speckle pairs appearing randomly distributed and separated over the speckle pattern; but, in fact, the speckle spatial separation and orientation frequency assessment of the speckle frame will show that the *most frequent* separation and orientation of speckle pairs will be representative of the observed binary star separation and position angle, though with a 180° ambiguity in position angle known as the phase problem (phase information is lost in the spatial assessment process because each speckle is assessed relative to every other speckle). The autocorrelation and subsequent Fourier transform of one speckle frame will produce a picture frequently referred to as the power spectrum of the image (see Fig. 12a), which is the sum of the sub-aperture diffraction-limited images, or speckle pairs, from around the speckle pattern. The power spectrum of the speckle image represents the power among the available spatial frequencies and orientations, and appears as a series of fringe pattern bands, the separation of which represents the separation of the binary star components (ρ), and the axis perpendicular to the fringe bands represents the position angle (θ) $\pm180°$.
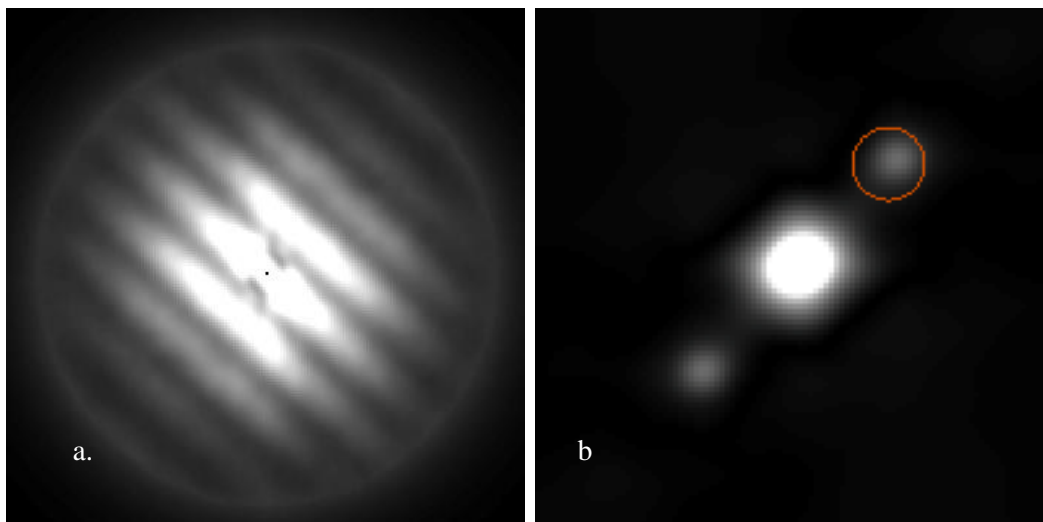
Fig. 12. (a) Power spectrum image: (average of 1000) of a series of speckle frames – the spacing of bands is inversely proportional to ρ, and the axis perpendicular to the bands reveals θ (180° ambiguity). (b) Autocorrelogram: created using general purpose astrometric software PlateSolve3 developed by Rowe of PlaneWave Instruments, with circle indicating solution to 180° position angle ambiguity determined by referencing previous astrometric measurements of the binary.

The astrometric measurements of θ ($\pm180°$) and ρ could be determined from the power spectrum of the speckle frame (knowing the pixel scale and camera angle – see below), however to define the binary star further, a Fourier transform can be applied again. The Fourier transform of the power spectrum of the speckle frame transforms the bands of the power spectrum into a sequence of three co-linear, circularized peaks with Gaussian profiles known as the autocorrelogram (see Fig. 12b). The Gaussian profile of the peaks aides in reduction efforts and determination of peak centers (Argyle 2012 pg. 266).

Completing the spatial frequency autocorrelation function for a series of speckle frames, for example 1000 per target, and averaging the power spectra computed for each of the 1000 speckle frames can further increase the reliability of the astrometric measurements θ and ρ. Additionally, deconvolution measures can be taken, including the incorporation of speckle information from bright single reference stars within the reduction process of general astrometry programs such as Rowe's PlateSolve3 (PS3) (Rowe & Genet 2014). According to Rowe & Genet (2014) deconvolution using bright reference stars (dividing the Fourier transform of the speckle images by the Fourier transform of single reference stars) will almost always sharpen the autocorrelogram image, and also remove much of the SNR reducing effects from telescope optical aberrations, including the effect of the central obstruction. Furthermore, if the imaged reference star and target binary maintain small spatial and temporal differentials, deconvolution will remove much of the atmospheric dispersion to the effects of seeing (see Fig. 13). Proper setting of Gaussian Highpass/Lowpass interference filters within the PS3 reduction process, to remove as much as possible the unwanted noise interference from electronics and the broad tail of the PSF due to seeing and optics, can further optimize the measurement of a binary star by boosting the SNR (Genet 2014b).
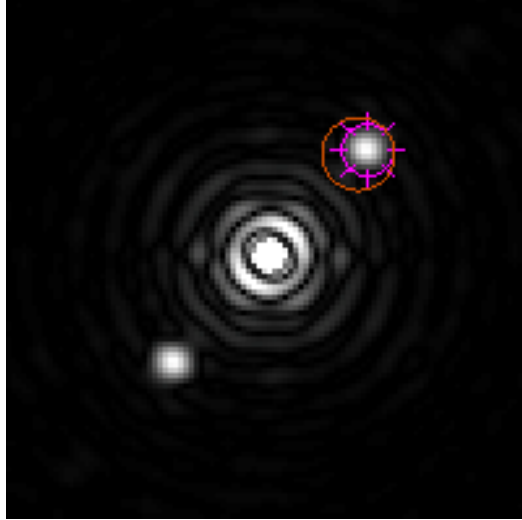
Fig. 13 – Autocorrelogram after deconvolution using a single bright, nearby (to the target) reference star from the Hipparcos catalog, further boosting SNR and defining the autocorrellogram.

Considerations of CCD Imaging &Speckle Interferometry Based Astrometry

Accurate determination of θ and ρ using images of binaries taken with CCD or EMCCD cameras, such as in speckle imagining described above, depends on knowledge of the scale and orientation of the image relative to the sky. The image or pixel scale (E) expresses the magnification of the image in arcseconds per pixel, and camera orientation angle (Δ) expresses the rotation of the CCD or EMCCD image relative to the celestial coordinate frame – the angle between celestial North and the X- or Y-axis of the image. E and Δ are the two scalar quantities which allow for translation of θ and ρ in the pixel coordinate frame (x,y) to the celestial coordinate frame. If the distance between two stars is R pixels, then their separation in arcseconds is:

$$\rho = E*R,$$

which is primarily a function of telescope focal length and the physical size of the CCD or EMCCD pixels. Δ is primarily a function of the CCD or EMCCD camera in the telescope's focus tube, and of the way the image is read, stored, and analyzed (Argyle 2012[16]). In general, most CCD or EMCCD software packages contain programs to view, reduce, and analyze

31

captured images, and these programs will enable the user to easily determine E and Δ either through the astrometric fitting method (matching image to a star catalog to determine RA and Dec of all stars in the image allowing for translation of pixel coordinate frame information to the celestial coordinate frame), or the method of pixel scale/image orientation (transformation of astrometric information between pixel and celestial frames using knowledge of image scale and camera orientation). If the camera is not moved, E and Δ will change little, if at all, between nightly observing sessions within a multi-night run, however calibration images and reductions of those images should be taken at the start of each observing session to insure these critical parameters have not changed.

Although speckle interferometry works well for resolving closely spaced celestial objects like binary stars, it does harbor observational limitations. For example, because speckle patterns are wavelength dependent, narrow band pass filters which reduce the total irradiance must be used to maintain a high degree of coherence to the patterns observed on the image plane, giving rise to magnitude limits (Hoffmann 2000; Mason & Hartkopf 2003). Speckle patterns are also subject to chromatic aberration (a function of zenith angle – see below) caused by the atmosphere, which can elongate speckles on the image plane, even with the incorporation of narrow band pass filters. This color dispersion effect can be mitigated using two crossed, shallow-angle Risley prisms, whose own dispersions vectorially add to cancel the atmospheric dispersion (Genet 2013). Moreover, to properly capture useable speckle pattern images, a sufficient high resolution, high speed, low noise imaging device is required, examples of which are traditionally very expensive, normally putting speckle techniques out of reach for ambitious amateurs. However, developments in the field of CCD and EMCCD cameras have made for some more affordable options, enabling speckle for anyone who can afford to pay a few hundred

dollars for a small, quality CCD camera or several thousand dollars for a quality EMCCD camera.

Horch (2006) describes the Δ magnitude (Δ mag.) problem – the difficulty in determination of the relative astrometry of the two stars in a very close binary system whose components have large magnitude differences. A CCD or EMCCD image of a star is a discreetly sampled pixelated version of the intensity point spread function (PSF) at the focal plane which depends on the size of the pixels and where the star is registered on the CCD array (see Fig. 14).

Unless the pixels are too large, accurate determination of an individual stars position from the intensity centroid of the samples PSF (near the brightest pixel) is not difficult (it is recommended that pixel size be smaller than the PSFs of stars to obtain well sampled images according to the Nyquist sampling principle). However, with two closely spaced stars, the PSF may overlap, or the PSF of the brighter star may completely blend with the fainter star's PSF, convoluting the centroid calculations and accurate determination of the stars' positions, and likewise the relative astrometry – see Fig. 15 (Argyle 2012[17]). One solution to the Δ mag. problem is known as PSF image modeling, and involves creating a mathematical model of two overlapping PSFs, then determining values for θ and ρ which minimize the difference between the math model and the actual image intensity distribution (Buchheim 2008).
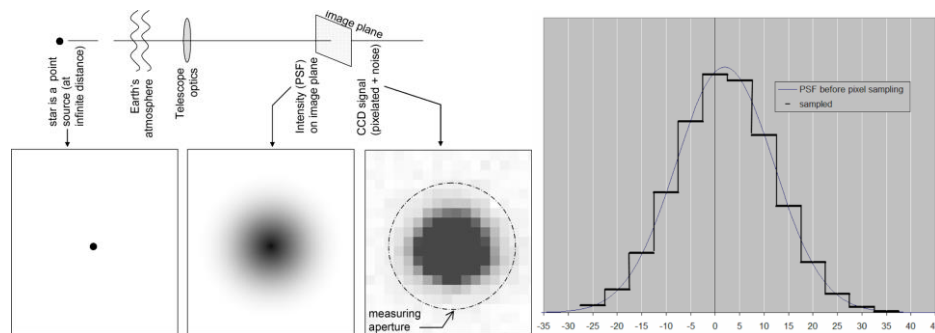
Fig. 14 – CCD Image Formation and PSF: (Left) The CCD's image of a star – the Point Spread Function (PSF) – is a blurred, discretely sampled intensity distribution, with random noise added. The center of the "brightest pixel" is not the best estimate of the star's position (right) (Buchheim 2008).

33
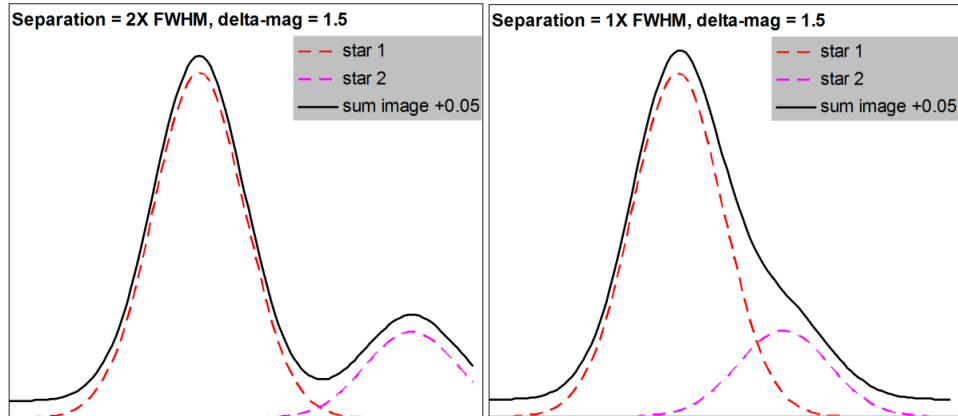
Fig. 15 – PSF formation of very close stars: Pairs of stars that are very close (right) do not display distinctly separate PSFs – the two stars become one merged image; whereas more separated stars form two distinct PSFs (right) (Buchheim 2008).

The refractive index inhomogeneity of the atmosphere is most prevalent at lower altitudes where the atmosphere is denser; thus, optical telescopes located at lower altitudes will suffer greater image break-up into speckles due to turbulent atmospheric cells than a telescope at higher altitude (Monnier 2003). The angle between the target and the zenith, representing the celestial target's altitude above the horizon, will also influence the atmospheric refraction which can impact measurements of some wider double stars, and is often recorded as air mass (how much atmosphere the starlight must traverse prior to arriving at the focal plane of a telescope). However, for altitudes greater than 30° (i.e. zenith angle < 60°) the effects of atmospheric refraction can be neglected. Closely spaced binaries will be even less affected by large zenith angles. Dispersion refers to the differential chromatic refraction of the atmosphere which is also a function of zenith angle wavelength – blue light refracted more than red light. This atmospheric effect can influence the astrometry of binary stars whose components exhibit greatly different peak emission wavelengths, as the refractive index will be different in magnitude and direction for each component. Considering these atmospheric effects, binary star imaging and observing for the purpose of making astrometric measurements should be restricted to zenith

angles less than 60°, below which special correcting filters would need to be employed (Argyle 2012[18]).

During the course of forming the autocorrelations from a series of speckle images and arriving at the full-aperture diffraction-limited fringe pattern of a binary, a 180° quadrant ambiguity regarding the secondary results from the loss of phase information. This phase problem is resolved by referencing previous observations of the binary in question, or through more advanced interferometry methods, such as the bispectral analysis technique (Hoffmann 2000).

Finally, the speckle interferometric method requires that the separation of the binary to be imaged must be on the order of 2-3 arcseconds or less for the entire image to fit within the isoplanatic patch. If the binary is too widely separated, light from each component will pass through different coherence cells so that each component image is subject to different aperture functions, creating differentials in the binary's θ and ρ values, which would not be suitable for autocorrelation analysis (Hoffmann 2000).

CHAPTER II
OBSERVATIONS

Equipment Details and Observational Conditions

Constructed in the early 60's, the National Optical Astronomy Observatory's (NOAO) 2.1-meter (84-inch) Cassegrain telescope at KPNO (see Fig. 14 & Fig. 15) was employed in the first major speckle interferometry program from 1976 to 1980 (McAlister & Hendry 1982). The 2.1-meter is equatorially mounted with an axis at 32°, and has a focal ratio of f/2.63 allowing for a relatively fast Cassegrain focus. With the f/7.6 secondary mirror in place, the effective focal length of the 2.1-meter during the Oct. 2013 observing run was 16,200 mm. The minimum angular separation of the 2.1-meter according to the Rayleigh criterion (see Chapter 1 – The Interference Phenomena of Light) is ~0.059 arcseconds. Considering the closest binary successfully resolved and accurately reduced during the Oct. 2013 run had an angular separation of just 0.074 arcseconds, it can be concluded that the employed speckle interferometry imaging system was effectively obtaining information near the diffraction-limit of the 2.1-meter.

Fig. 16 – NOAO 2.1-meter telescope housing complex at KPNO: The multi-story housing complex of the NOAO 2.1-meter telescope at KPNO (center) and auxiliary 0.9-meter telescope housing (left) which formerly provided the feed for the Coude spectrograph instrument in the lower level of the building.

Fig. 17 – The NOAA 2.1-meter Telescope at Kitt Peak National Observatory: pictured here with a KPNO staff member installing lead counterweights to balance the telescope. Note black secondary mirror housing above and white flat screen in background used in calibration.

Effective speckle interferometry of close binary stars requires the ability to obtain many short exposures, on the order of tens of milliseconds, of close binary stars using a telescope with resolution capabilities sufficient to separate the components of target binary stars. To meet the requirements of fast, high SNR imaging, an EMCCD camera can be employed. An EMCCD camera, through electron multiplication of the signal prior to the charge-to-voltage conversion, amplifies the signal noise by applying a high voltage to render insignificant the noise resulting from the device's high speed frame-transfer capabilities (Genet 2013a). A regular CCD camera would be able to make short exposures, but would prove highly inefficient in a situation where 1000 short exposures of a target in series is the standard.

During the observing run described in this thesis, an Andor Luca-R EMCCD camera-based speckle imaging system (see Fig. 16 & 17) was interfaced with the 2.1-meter telescope. The Luca-R camera, with a 1004 X 1002 pixel array and 8 micron pixel size, in conjunction with a 2 inch x2 OPT Barlow in front of a Moonlite focuser, and a 2-inch x4 TeleVue PowerMate after the focuser to give a total magnification of x8, comprised Genet's (2013a) portable speckle

imaging system. An Orion 5-position filter wheel immediately preceded the Luca-R camera, and all observations were made through a Sloan i' narrow band pass filter while targets were as close to the meridian as possible to reduce atmospheric dispersion. The triangular Luca-R camera is small and relatively lightweight, being 40cm long (along each of the three long axes), 20cm wide, and roughly 3 kg. Although back-illuminated EMCCD cameras, in which the CCD chip is not protected by gate structures which attenuate incoming radiation as in front-illuminated cameras, offer higher quantum efficiencies (QE ~ 90%), that is, the efficiency in which the CCD chip converts photons into electrons, the benefits of the front-illuminated Luca-R model EMCCD camera (QE ~50%) including lower cost (under 15K USD), much lighter weight, USB access, and overall better portability, were thought to be worth the loss of quantum efficiency (Genet 2013a & 2014b). The Luca-R EMCCD camera was used to obtain multi-plane FITS data cubes of the target binaries, each consisting of 1000 20 ms exposure speckle images. Given the quantity and exposure time, typical integrations were just a few minutes per target.

Interfacing Genet's speckle imaging system to the 2.1-meter was relatively simple through the use of a previously used ½ inch thick aluminum back plate for instrumentation integrations with the 2.1-meter's acquisition/guider unit (see Fig. 16). The focuser on the Luca-R camera was set to be parafocal with the acquisition/guider unit's camera through the use of a Moonlite motorized focuser. Control of the Luca-R camera and motorized filter wheel from the warm room was enabled through the use of a 50-foot Cat 5 Ethernet cable running from an Icron Ranger 2204 USB extender. NOAO supplied instructions for interfacing guest computers with the 2.1-meter control computer so that direct logs of telescope pointing, truss temperature, and other information could be recorded alongside individual target observations. Genet's speckle camera system, with a total magnification of x8, provided an overall effective focal length of

about 129,600 mm, and a focal ratio of f/61.7 when integrated with the 2.1-meter. With the

Luca-R's 8-micron pixel size, the pixel scale (E) was determined to be 0.0125 arcseconds/pixel

(more on this determination in Chapter 3).
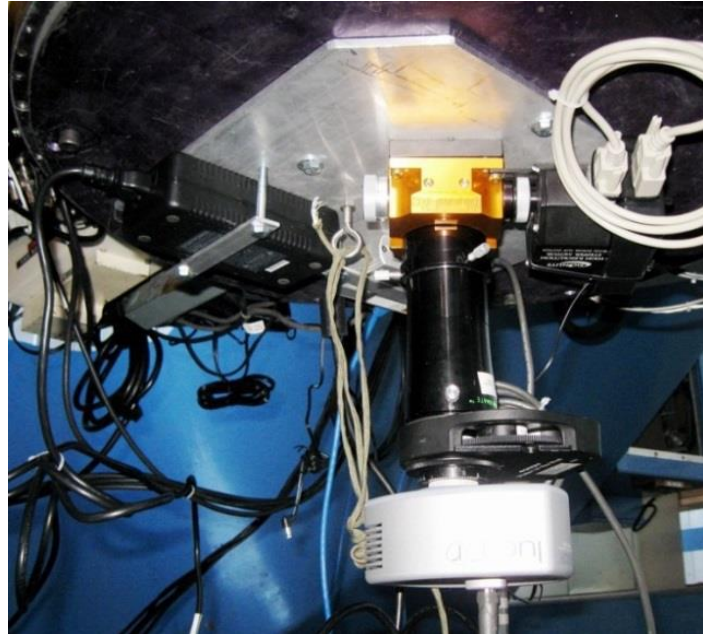
Fig. 18 – Genet's portable speckle camera system fully interfaced with the 2.1-meter telescope. The speckle camera system consists of: a motorized Moonlite focuser, Hyperion Magnifier (in practice a series of x2 and x4 2-inch Barlow lenses), Orion seven-position motorized filter wheel, Andor Luca-R EMCCD camera, and Icron Ranger USB extender. The speckle camera system was controlled from the warm room via a 50ft CAT-5 Ethernet cable.
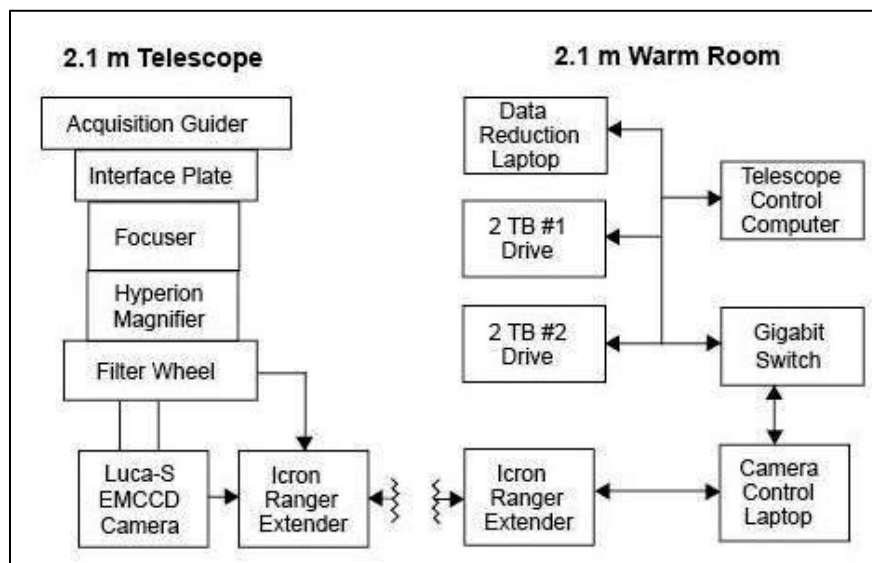
Figure 19 – Genet's portable speckle imaging system block diagram (Genet 2013a).

Observational Targets

The Oct. 2013 speckle run at the 2.1-meter produced a database of raw speckle images (stored as FITS files) totaling 1.4 terabytes composed of 1071 binary star multi-plane FITS data cubes, as well as 134 single reference star data cubes obtained for deconvolution within PS3 speckle reduction. Each individual close binary star FITS cube contained 1000 individual speckle images, each image representing a 20 millisecond EMCCD exposure of the target (some targets were imaged more than once). The FITS cubes were organized into an Excel spreadsheet and Microsoft Excel CSV files by student co-investigator Teiche for use in subsequent PS3 preprocessing and reduction (Teiche et al. 2014).

Genet (2014b) describes the five classes of double stars which composed the initial target list of over 500 different double stars, calibration binaries, and deconvolution single reference stars for the entire nine-night Oct. 2013 speckle run on the 2.1-meter. Most of the proposed targets for the run fell under the class titled *Known Binaries with Published Orbits*, including the six target binaries investigated in the current work. The WDS identification, location, magnitude data, and near term ephemerides (2013-2015) for the six target stars pertaining to this thesis are summarized in Table 1 below.

Table 1. Summary of target binary stars: WDS identifier, location (RA Dec), component magnitudes (V1 = Primary Magnitude, V2 = secondary magnitude), and near term ephemerides (θ = position angle in degrees, ρ = angular separation in arcseconds). (USNO 2015a)

WDS	RA	Dec.	V1	V2	θ 2013	ρ 2013	θ 2014	ρ 2014	θ 2015	ρ 2015
19069+4137	190656.22	413719.6	9.1	9.1	292.8	0.183	284.1	0.176	274.7	0.168
22357+5413	223539.4	541324.1	8.5	9.1	288.1	0.145	291.8	0.152	295.3	0.159
05153+4710	51515.45	471014.6	7.2	9.1	99.1	0.44	99.8	0.444	100.6	0.448
06256+2227	62534.2	222728.2	7.3	9.4	260.3	0.575	260.6	0.578	261	0.58
02231+7021	22304.7	702035.6	8.4	8.7	140.5	0.473	139.6	0.459	138.7	0.444
04505+0103	45027.32	10300.5	9.2	10	233.5	0.207	231.6	0.202	229.7	0.198

The six target binaries, classified by Hartkopf et al. (2001) as bad orbit binaries (USNO orbit grade 5.0), were selected from the KPNO I run master target list compiled by Genet et al. (2014b). The targets were purposely selected based on their respective USNO orbital plot diagrams, where recent clear deviation from the previously published orbit was evident from recent speckle observations, and perhaps an additional speckle observation might resolve whether the recent observations were anomalous or indicative of a developing trend, signifying a need for orbital revision or even reconsideration of binarity altogether in certain cases. The six targets are not unique in this respect among stars in the WDS. Indeed, as of 2015 according to the USNO, 18,624 WDS double stars are known to be physical binaries, while 4,293 are known to be optical pairs, representing ~15% and ~3.5%, respectively, of the entire catalog. Thus, the true natures of the vast majority of systems in the WDS are still undetermined (USNO 2015a).

The current USNO orbit grading scheme is a modification of the evaluation scheme used by Worley & Heintz (1983) in the Fourth Catalog of Orbits of Visual Binary Stars (hereafter Fourth Catalog). The Fourth Catalog orbit grading scheme was based on orbital coverage, number of observations, and the overall quality of the observations. The Fourth Catalog grade was presented on a numerical scale (1=definitive to 5=indeterminate). Worley & Heintz (1983) used their collective double star experience of over six decades to make their qualitative assessment of individual observers, and thus their grading system was quite subjective.

Within the most recent orbit catalog, the Sixth Catalog of Orbits of Visual Binary Stars (hereafter Sixth Catalog), Hartkopf et al. (2001) have developed a more objective grading scheme based on the same grading criteria used for the Fourth Catalog. Using a very large sample size of observations corresponding to well-known orbits, Hartkopf et al. (2001) evaluated the observations, considering factors such as telescope aperture, number of nights of observing,

expertise of the observer, technique, and other factors. These evaluations of observations were then used to help assess many of the same orbits from the Fourth Catalog. Factors considered in the Sixth Catalog grading include total number of observations, position angle coverage, and number of revolutions from first to last observation, among others. The modified grading scheme for the Sixth Catalog consists of grades on a numerical scale from 1.4 – 5.0. Descriptions associated with orbit grades remain as they did in the Fourth Catalog. For example, a Sixth Catalog orbit grade of 1.4 corresponds to an orbit described as having well-distributed coverage exceeding one revolution; no revisions expected except for minor adjustments (Worley & Heintz 1983). All six targets of the current study correspond to Sixth Catalog orbital grades of 5.0, and are described as an orbit whose elements may not even be approximately correct, the observed arc is usually too short, with little curvature, and frequently there are large residuals associated with the computations (Worley & Heintz 1983).

Table 2. Most recent WDS observational data for the observed target stars.
Observational Technique Codes: S = speckle interferometry, Su = USNO speckle.
(USNO 2015a)

WDS	Epoch	θ (°)	ρ (")	Telescope Aperture (m)	Author	Observation Technique
02234+7021	2010.053	140.1	0.651	1	Pru2012	S
04505+0103	2010.0653	252.3	0.294	3.8	Msn2011d	Su
05153+4710	2008.066	97.6	0.368	2.1	Gii2012	S
06256+2227	2008.8882	256.7	0.72	1	Orl2009	S
19069+4137	2008.563	348.1	0.211	0.7	Gii2012	S
22357+5413	2008.639	180.3	0.254	0.7	Gii2012	S

Mason (private communication, 2014) of the USNO, has supplied all WDS and Sixth Catalog data for the six target binaries (see Table 13 in Appendix C), and agrees that recent observations show significant deviations from published orbits, indicating that the published orbits are in need of revision. The USNO orbital plots for the six target binaries can be found in Fig. 37 in Appendix B. Within the plots, the dashed line indicates the line of nodes, all scales are

in arcseconds, the plus sign at the origin indicates the location of the primary star, the bold black line represents the computed orbit, and the curved arrow at lower right indicates the direction of celestial north and orbital motion of the secondary star. Identifiers and the reference codes for the orbit computation work are also shown on these diagrams. See Fig. 6 on page 14 for further explanation of USNO orbital plots. The computed orbital elements for each target binary are given in Table 13 in Appendix C.

CHAPTER III
METHODS

PS3 Data Reduction

The entire 1.4 terabyte collection of 1071 multi-plane FITS cubes, each containing

approximately 1000 raw 20 millisecond exposure speckle images for each target observed

throughout the Oct. 2013 KPNO I speckle run, was reduced exclusively using the general

astrometry software program PlateSolve3 (PS3) (Rowe & Genet 2014). PS3's automatic

preprocessing feature was utilized to reduce the large 1.4 terabyte dataset into a more

manageable 1.5 gigabytes. Preprocessing was completed in approximately 24 hours using a

Windows-7 machine with a 2 GHz processor. The preprocessing of one typical FITS data cube

of 1000 raw speckle images is completed in approximately two minutes, during which time the

Fourier transforms of all 1000 speckle images that comprise a data cube are obtained, followed

by the averaging of these transforms to produce one average power spectrum image as described

in Chapter 1. A single power spectrum image is referred to as the power spectral density fringe

pattern, or PSD, within the PS3 program, and corresponds to a file size of approximately 1

megabyte. Aside from creating a more manageable dataset, preprocessing the raw speckle image

data cubes also allowed for faster reduction of the target binaries within the PS3 speckle

reduction process.

As described in Chapter 1, the Fourier transform of the power spectrum image results in

the autocorrelogram image, which can be focused and sharpened using the Gaussian Lowpass

and Highpass filter features and reference star deconvolution features of the PS3 program. The

Gaussian Lowpass filter is applied to the PSD, with a cutoff proportional to the spatial frequency

of the Airy disk (see Chapter 1), fc (in pixels) given by:

$$fc = (hN) / (2.44 \, \lambda \, F/D),$$

where h is the pixel dimension in microns, N is the size of the image in pixels, and F/D is the

focal ratio of the optical system (focal length of telescope in mm divided by aperture diameter in

mm). This allows for improved SNR and reduction of unwanted interference from the

electronics, the sky background, and from photon shot noise of the object – see Fig. 19. Use of

the Gaussian Highpass filter, although not usually needed if reference star deconvolution

measures are taken, removes the lowest-frequency information of the image to diminish the

broad tail of the PSF which is due to seeing and optics – see Fig. 20 (Genet et al. 2014b).
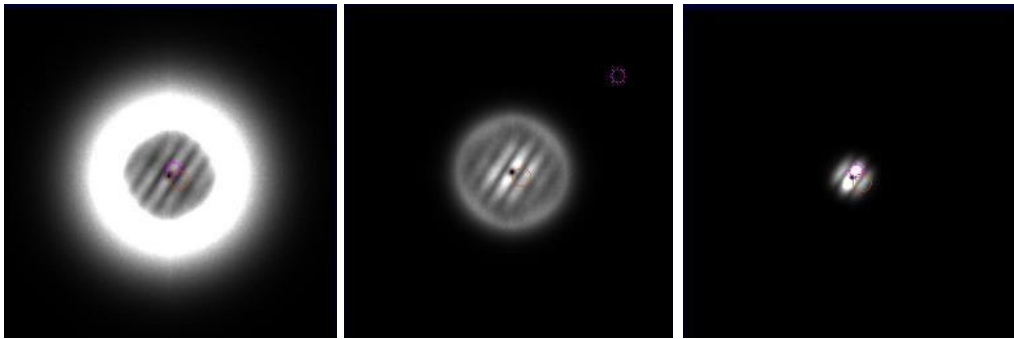
Fig. 20 – PSD Gaussian Lowpass Filter Setting. Left – the Gaussian Lowpass filter cutoff is set beyond fc, allowing high frequency noise to be included. Right – setting is too narrow, cutting off useful signal information. Center – the filter is set effectively, cutoff being slightly larger than the Airy disk spatial frequency imposed by the telescope's aperture. (Genet et al. 2014b)
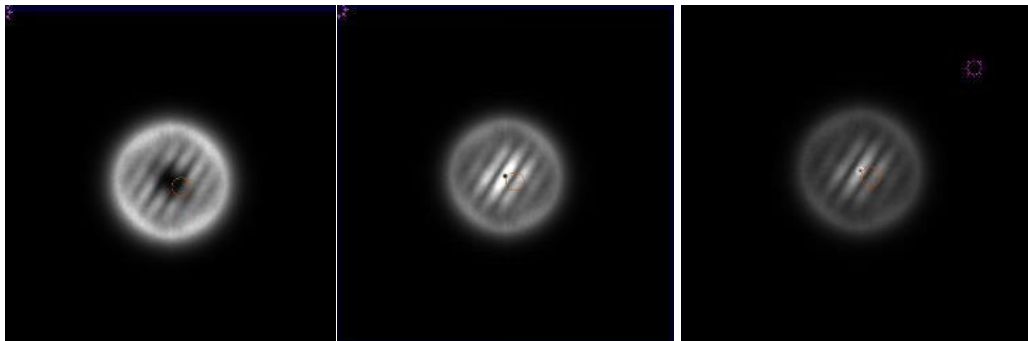
Fig. 21 – PSD Gaussian Highpass Filter Setting. Left – the Gaussian Highpass filter is set too wide, not only cutting out the bright central peak, but also much of the fringe pattern. Right – the filter is set too narrow, allowing the bright central peak to shine through. The center setting is effective.

Use of the Gaussian filters, when set effectively, can optimize the detection and measurement of a target double star. The Gaussian Lowpass and Highpass filter settings for the PS3 reductions of the Oct. 2013 speckle observations, including the six target binaries of the current work, were set at 35 pixels and 2 pixels respectively.

Deconvolution using reference star speckle images taken periodically throughout an observing run can also aid in sharpening the autocorrelogram by removing much of the telescope's optical aberrations, the atmospheric dispersion, and broad tail due to the effects of seeing. PS3 uses speckle images of single reference stars to estimate, in Fourier transform space averages, the image degradations from the telescope and instantaneous atmosphere characteristic of a given time and observing region in the sky, which are then divided into the actual image recorded to produce an image with telescope and atmospheric distortions removed - symbolically:

$$\langle O \rangle = \langle I \rangle / \langle T \rangle,$$

where $\langle O \rangle$ is the average of the Fourier transform of the image without telescope and atmospheric distortions, $\langle I \rangle$ is the average of the Fourier transform of the recorded image, and $\langle T \rangle$ is the average Fourier transform of the PSF of the telescope plus instantaneous atmosphere.

Table 3. WDS identifiers of the six target binaries and associated reference star HIP numbers. Reference stars were observed often throughout the run to preserve small spatiotemporal differentials relative to target binaries for optimal deconvolution with PS3. RA diff. given in 0hr:00min:00.00sec.

Target Binary	Associated Ref. Star	RA Differential	Dec Differential
19069+4137	HIP100587	1:17:35.40	9°26'35".00
22357+5413	HIP113498	0:24:09.60	5°35'28".70
05153+4710	HIP31665	1:22:22.94	9°41'12".50
02231+7021	HIP2599	2:30:44.71	8°05'21".20
04505+0103	HIP7884	3:09:01.43	4°26'14".90
06256+2227	HIP19205	2:18:33.74	7°13'16".60

Optimally, the single reference stars to be used in the deconvolution process described by Rowe & Genet (2014) should be bright enough to maintain high SNR after speckle preprocessing, and be as near as possible to the target double star in both time and space (Genet et al 2014). As can be seen in Table 3 above, which lists the six target binary stars along with the associated single reference stars, no reference star used for deconvolution was more than approximately 45.15° away from a target binary (1hr RA = 15°). The mean RA and Dec position differentials for reference stars relative to target binaries were calculated to be approximately 28° and 7.4° respectively.
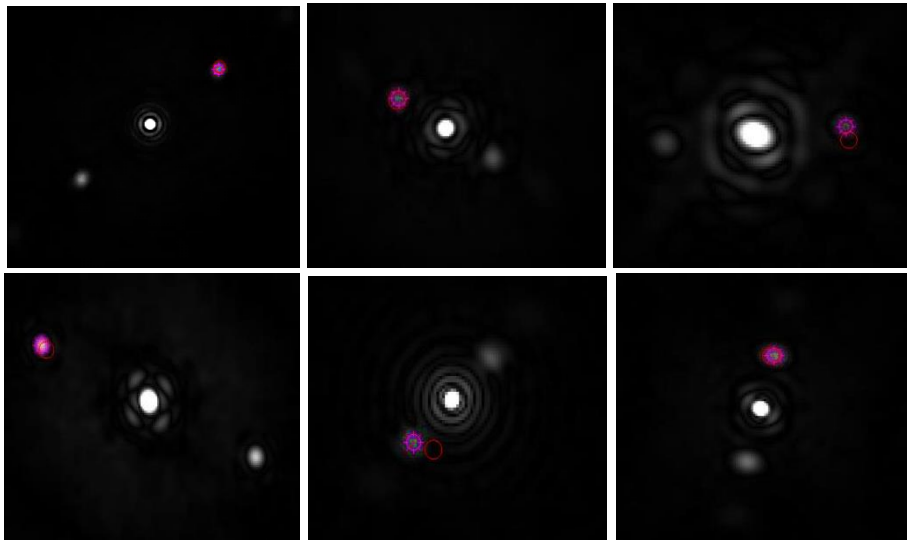
Fig. 22 – Autocorrelograms for the six target binary stars. (Read top to bottom, L to R): WDS02231+7021, WDS04505+0103, WDS05153+4710, WDS06256+2227, WDS19069+4137, and WDS22357+5413. Note well-structured Airy disks of primary stars in center of autocorrelograms, red circles indicating solution of 180° phase ambiguity, as well as pink circle with radials representing PS3 centroid lock-to-peak astrometry tool.

As a solution to the phase problem inherent to speckle interferometry, PS3 incorporates the expected values for secondary position angle based on projected θ and ρ ephemerides or the last observed position angle on record, and indicates this solution by placing a red circle which may partially encompass or at least fall near the correctly located secondary in the

47

autocorrelogram image. Following satisfactory production of the autocorrelograms of the six

target binaries (see Fig. 22 above), the astrometric measurements (θ and ρ) for each system were

obtained using the PS3 Astrometry control panel within the speckle reduction suite (see Fig. 23).
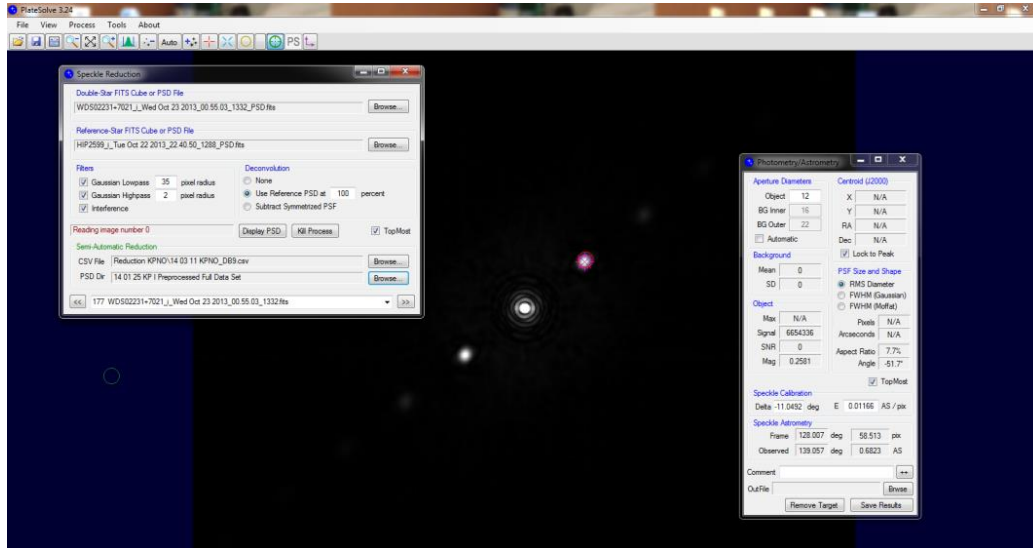
Fig. 23 - The speckle reduction GUI control panels of PS3 displayed during reduction of WDS02231+7021. The panel on the left allows the user to input data files for reduction in manual or semi-automatic modes, set Gaussian highpass/lowpass filters, and deconvolution parameters. The panel on the right allows the user to control the size of the centroiding circle among other parameters, adjust camera angle and pixel scale if necessary, and displays the astrometric solutions.

With the bright primary star at the exact center of the image when viewing the

autocorrelogram, PS3 can automatically detect and lock-on to the pixel locations of the centroid

of the appropriate secondary image, or allow the user to manually accomplish this if the

automatic solution is not satisfactory. Once the secondary centroid has been effectively locked,

the relative astrometry of the binary as viewed in the image plane is trigonometrically

determined. With accurate camera angle and pixel scale information, the image plane astrometry

(θ and ρ) is converted to that of the celestial plane – the true observed astrometry of the target

binary. To arrive at the true position angle, the camera angle, which is determined by observing

and reducing calibration binaries outside of the general reduction process (described below), is

subtracted from the image frame position angle. To arrive at the true separation, the image frame

separation in pixels is multiplied by the pixel scale constant (arcseconds/pixel), which has also been determined through a previously executed calibration process. Below, Table 4 summarizes the newly determined astrometric measurements for the target binaries, as well as the most recent cataloged astrometric measurements and the predicted measurements based on published ephemeris.

Table 4. Summary of PS3 reduction data for the six target binaries. Columns from left to right are: WDS Identification, the observed position angle, the most recent cataloged position angle, the predicted position angle based on published ephemerides, the difference between the observed position angle and the predicted position angle, the observed separation, the most recent cataloged separation, the predicted separation based on published ephemerides, and the difference between the observed and predicted separations.

WDS Target	$\theta_{Obs.}$ (°)	$\theta_{Cat.}$ (°)	$\theta_{Ephem.}$ 2013	$\theta_{O\text{-}Ephem.}$ (°)	$\rho_{Obs.}$ (")	$\rho_{Cat.}$ (")	$\rho_{Ephem.}$ 2013	$\rho_{O\text{-}Ephem.}$ (")
19069+4137	325.49	348	292.8	32.69	0.225	0.2	0.183	0.042
22357+5413	177.04	180	288.1	-111.06	0.306	0.3	0.145	0.161
05153+4710	106.31	98	99.1	7.21	0.390	0.4	0.44	-0.050
02231+7021	139.03	140	260.3	-121.27	0.684	0.7	0.575	0.109
04505+0103	249.83	252	140.5	109.33	0.298	0.3	0.473	-0.175
06256+2227	256.06	257	233.5	22.56	0.738	0.7	0.207	0.531

The new astrometry data for the six target binaries is in good agreement with the most recent, or last cataloged astrometric observations and measurements, which for all targets was a previous speckle observation (see Figure 37 in Appendix B; Table 2 on page 41). This agreement preliminarily indicates good accuracy of the new astrometric measurements, as the recently published speckle measurements, especially that of USNO are typically considered to be highly accurate. Large differences between the observed and predicted values for both θ and ρ are likely the result of prematurely published ephemerides computed from preliminary orbits which inaccurately describe the systems of the targets. Previously unresolved quadrant ambiguities in the cases of targets with very similar component visual magnitudes could also account for some of the very large observed-predicted θ values.

Calibration Process

As described previously, accurate determination of the speckle imaging system camera angle (Δ) and pixel scale (E) values are necessary to transform the image frame separation and position angle in pixels to the true observed separation in arcseconds and position angle in degrees within the celestial plane. A few methods exist for such determinations, including for example the use of a full-aperture slit mask to produce a fringe pattern of a bright star whose fringe spacing can be translated to the image scale in arc seconds per pixel, assuming split spacing, distance between the focus and mask, wavelength and f/number are known (Hoffman 2000). A common and well-attested method for determination of camera angle, known as the drift or star trail method, involves pausing the telescope drive and allowing a star to drift diurnally across the field of view such that an east-west line is evident, allowing the direction of celestial north to be found and the image orientation determined when the image is compared to a calibration binary image with well-known θ and ρ. Moreover, if the field of view includes enough stars, then one could choose from a host of different astrometry programs which employ astrometric fitting methods to determine Δ and E. Astrometric fitting involves comparing the RA and Dec coordinates of every star in the image to known values published in recent stellar atlases and position catalogs. If a well populated globular cluster could be viewed, then one could determine the camera angle and pixel scale by imaging the globular cluster and comparing against a matching astrometry image taken by the HST.

For various reasons, none of the above methods were chosen to determine the Δ and E values for the Oct. 2013 KPNO I speckle run observations. A full-aperture slit mask was considered and rejected due to manufacturing and transporting difficulty. Likewise, a sub-aperture slit mask for the secondary mirror was also considered and rejected because the

telescope's dimensional uncertainties would have been too great (Genet 2013a). The drift

calibration method was attempted during the engineering checkout night prior to the official start

of the run, but due to the very narrow field of view characteristic of Genet's speckle camera

system integrated with the 2.1-meter (12.6 x 12.5 arcseconds), the drift method was not practical

as stars passed through the field of view much too quickly (approximate .8 sec) to provide usable

calibration data. The astrometric fitting method was also not an option due to the very narrow

field of view, as no other stars appeared in the image plane except the target. The globular

cluster plate solve method was attempted during a speckle run six months after the Oct. 2013 run

during KPNO II, but without success, because locating and matching a suitable cluster proved

too time consuming.

Prior to the run, it was decided to follow in the footsteps of McAlister & Hendry (1982)

and use observations of binaries with published orbits and ephemerides in a comparative analysis

against observed measurements of position angle and separation to determine Δ and E. This

analysis was performed initially as a quality check near the beginning of the run, using the

astrometry program REDUC to reduce the initial observed binary star data and determine the

observed position angle and separation. Position angle and separation observed minus calculated

(O-C) values were determined, and initially theses values showed large distribution from one

binary to the next. After some thought, it was soon realized that such distribution, which would

typically indicate something was wrong within the imaging system or reduction process, was

normal and even expected, as many of the initial observed binaries reduced for the quality check

had poorly described orbits by USNO standards, thus the observations were not necessarily off.

Indeed, even the five calibration binaries chosen (see Tables 11 and 12 in Appendix A) had an

average USNO orbit grade of 4.2 – a grade that represents a preliminary orbit due to orbits with

less than half the ellipse defined by the observational records, weak or inconsistent data, or

evidence of orbits showing deteriorating representations of recent data. Specifically, four of the

calibration binaries (WDS01532+1526, WDS23595+3343, WDS04041+3931, and

WDS03122+3713) maintain observational records that span less than half of the computed orbit.

It should be noted however, that the data thus far for these systems fit relatively well to the

computed orbits (see Fig. 36 in Appendix A), and thus they were deemed acceptable for

calibration. Use of binaries with much better USNO orbit grades for calibration would have

been preferable; however such binaries which have observational histories covering the full orbit

are typically extremely close pairs with orbital periods on the order of tens of years, and as such

were beyond the resolution limits of the KPNO I system. A more refined and robust camera

angle and pixel scale calibration process then the previously mentioned initial attempt was

carried out after the Oct. 2013 observing run by the author, using a total of 274 speckle

observations of the five calibration binaries to determine the differences between the observed

and predicted ephemeris values for position angle and separation. From this calibration process,

Δ and E were determined to be -11.013° and 0.0117 arcseconds/pixel respectively. The averages

of observed position angles in image frame pixels and observed separations in image frame

pixels for each calibration binary were used along with the respective published ephemerides to

determine the camera angle (equation 2) and pixel scale (equation 1) according to the following

equations:

$$\sum_{i=1}^{5} (\rho_{\text{Ephem}.i} - \rho_{\text{Obs}.i} * E) = 0 ....(1)$$

$$\frac{1}{5}\sum_{i=1}^{5} (\theta_{\text{Obs}.i} - \theta_{\text{Ephem}.i}) ....(2)$$

Following the Oct. 2013 run, reconsiderations regarding the use of ephemeris data based

on published orbits to determine Δ and E through comparative analysis means, as well as

perform general calibration analysis described below, led to consideration of an alternate

calibration method involving maximum likelihood predictions (MLP) for θ and ρ, calculated

from a least squares fit to recent speckle observations from the USNO 4th Interferometric Catalog

(hereafter 4th catalog). The argument for the MLP calibration method can be understood when

one considers that there is an inherent conflict between a mathematically derived orbit that best

fits the entire observational record versus a mathematical prediction of θ and ρ of a single

observation not far in the future. Perhaps one would be better off not using published

ephemerides for calibration, but some other analytic technique to forecast θ and ρ values for the

night of observation. It was decided then to take the four most recent speckle observations for

each calibration binary from the 4th catalog, and use these to create artificial ephemeris values, or

MLP values for use in calibration. The author has determined the MLP values for the calibration

binaries corresponding to the median observation night date (2013.8027) and compared these to

all observed position angle and separation values of the calibration binaries. The O-C position

angle and separation mean values for all 234 observations representing four calibration binaries

using the MLP method described above produced new Δ and E values of -11.226° and 0.01224

arcseconds/pixel. It should be noted that in the original calibration method using ephemeris data,

274 observations were used, representing five different calibration binaries; however

observations of calibration binary WDS01523+1526 were ignored within the MLP method due

to position angle O-C values which were largely inconsistent with the same values from the rest

of the calibration binary observations.

Application of the MLP method determined calibration values to the observed calibration

binary measurements in image frame pixels to arrive at the true observed position angles and

separations yielded mean O-C values for position angle and separation of 0.5038° ($\sigma = 0.334°$,

$\sigma_{\bar{x}} = 0.0218°$) and 0.0404″ ($\sigma = 0.0315″$, $\sigma_{\bar{x}} = .0021″$) respectively. The MLP values for camera

angle and pixel scale were expected to be more accurate and thus produce smaller mean O-C

values for position angle and separation than those produced using the published ephemeris data,

as they represented a camera angle and pixel scale calibrated to predicted values from recent

speckle observations in which calibration was carried out using more accurate methods (slit

mask, etc.), rather than calibration against ephemerides stemming from published orbits intended

to be a best fit to all recorded observations, including lower accuracy observations. However,

comparison of all calibration binary O-C values, including σ and $\sigma_{\bar{x}}$ values, revealed that the

camera angle and pixel scale values determined using the published ephemerides yielded slightly

more accurate results than those determined using the MLP method. Specifically, application of

the original ephemerides method determined calibration values to the observed calibration binary

measurements yielded mean O-C values for position angle and separation of 0.4138° ($\sigma =$

0.2333°, $\sigma_{\bar{x}} = 0.0141°$) and 0.0147″ ($\sigma = 0.0087″$, $\sigma_{\bar{x}} = .0005″$) respectively. There is an ongoing

investigation by the author and Genet as to the best method and treatment of data for the

determination of camera angle and pixel scale calibration values.

The 274 calibration binary observations were obtained by imaging each calibration

binary (see Appendix A Tables for WDS identifiers of the four calibration binaries) close to the

meridian approximately ten times in an uninterrupted series during nearly every night over the

course of the run. Observing the calibration binaries near the start of the run and several times

per night throughout the run in this manner provided the necessary data to estimate the

aforementioned camera angle and pixel scale, and also for the statistical assessment of the

within- and between-night internal precision and overall precision of the observations, as well as

an estimate of the overall accuracy of the observations as compared to the ephemeris θ and ρ values.

To assess the overall precision of the current work's observations and those of the entire Oct. 2013 observing run, the mean (μ), standard deviation (σ), and standard error ($\sigma_{\bar{x}}$) of the mean were found for all observed θ and ρ values in image frame pixels of the five calibration binaries made throughout the entire run. An estimation of the precision of observations within and across nights was also determined using standard deviation values of θ and ρ measurements in image frame pixels within specific nights and across nights.

To provide an estimate of the overall accuracy of the observations, as well as an estimate of the within and between night accuracies, the same statistical analysis methods were applied to all θ_{O-C}, and ρ_{O-C} values; but there is, of course, a degree of circularity in using the same set of binaries to not only determine the camera angle and pixel scale, but to also make an external accuracy estimate (regression toward the mean). The accuracy estimate may thus be an underestimate. On the other hand, since the accuracy estimate includes both observational errors and errors in the orbital position predictions, it may be an over-estimate (Genet, private communication, 2014). Based on a sample of 274 speckle observations (each containing 1000 individual speckle frames) split between the five calibration binaries, the overall internal precision (σ) of θ and ρ observations made during the Oct. 2013 KPNO I speckle run was determined to be 0.027° ($\sigma_{\bar{x}} = 0.0116°$) and 0.00226 arcseconds ($\sigma_{\bar{x}} = 0.00068''$) respectively. Within and between night precision (σ) for position angle observations was determined to be 0.013° and 0.026° respectively. Within and between night precision (σ) for separation observations was determined to be 0.00197 arcseconds and 0.00228 arcseconds respectively.

Better precision within nights was expected as temperatures and other factors change slightly between nights.

The overall accuracy (σ) of θ and ρ observations made during the Oct. 2013 KPNO I speckle run was determined to be $0.4138°$ ($\sigma = 0.2333°$, $\sigma_{\bar{x}} = 0.0141°$) and $0.0147''$ ($\sigma = 0.0087''$, $\sigma_{\bar{x}} = .0005''$) respectively. Within and between night accuracy (σ) for position angle observations was determined to be $0.013°$ and $0.0262°$ respectively. Within and between night accuracy (σ) for separation observations was determined to be 0.00064 arcseconds and 0.00213 arcseconds respectively. As with precision, within night accuracies were expected to be better than between night accuracies. The statistical analysis of the five calibration binaries from which the precision and accuracy estimations were derived is summarized in Tables A.1 and A.2 of Appendix A.

CHAPTER IV
RESULTS & DISCUSSIONS

Analysis

Observations of the relative astrometry of visual binary stars over time are necessary for

effective interpretation of the system, calculation of the apparent orbit, and derivation of the true

orbital parameters. In its most basic sense, orbital analysis consists of confirming the binary

nature of a system based on a record of observations that reflect the movement of the double star

components relative to each other. For example, a plot of obtained astrometric measurements for

θ and ρ against time which exhibits a good fit to a parabolic curve or fraction thereof could

indicate binarity (Keplerian motion). However, if the same type of data plot showed a better fit

to rectilinear motion, then the components may not actually represent that of a gravitationally

bound binary, although alternate conclusions based on the same plot could be a binary system

observed edge-on, as is the case with ε Aurigae – an eclipsing binary that exhibits eclipses ever

27 years, or a very long period binary system where the small fraction of observed orbit is so

small it appears as basically a straight line. In the case of an edge-on system, visual observations

spanning at least half of the orbit, showing movement of the secondary along the axis tangent to

the line-of-sight, or photometric observations of periodic dimming indicating an eclipsing binary,

or spectroscopic observations would be necessary to confirm binarity. Observations and

measurements of binaries throughout a complete orbit are not necessary to complete this most

simple of orbital analysis; however most astrometrists stress the importance of a significant

portion of the orbit being observed prior to making any definite conclusions. This point is moot

regarding widely separated binaries with very long orbits whose entire observational history may only cover a small fraction of the possible orbit. Indeed, the geometry of many binaries has changed little in the past two centuries. Presented below are the USNO WDS observational data records (including the author's new speckle measurement) for the six target binaries and the associated plots of position angle and angular separation vs. epoch for each target (see Tables 5 – 10 and even-numbered Figs. 24-34). Within the observational records were photometry observations which contained no θ and ρ values, and thus were ignored during interpretation of the data. Data with incomplete astrometric measurements were also not considered in this investigation.

Also presented below are the updated USNO orbital plots for each of the six target stars, which have been revised to reflect the new astrometric measurements of the current work, along with O-C lines, observational method keys, primary and secondary magnitudes, and the period, semi-major axis, and approximate computation date of the previously published orbit (see odd-numbered Figs. 25-35). The descriptions and interpretations of these plots remains as previously explained in chapters 1 and 2. In the case of WDS19069+4137, the previous observations were identified in order to simplify interpretation of this binary.

WDS19069+4137

An orbit of 41.6 years was published for WDS19069+4137 by Couteau (1999), after eight visual measurements and three interferometric-type measurements. These interferometric measurements appear to be outliers, made using a so-called photoelectric phase-grating interferometric technique described by Tokovinin (1985). Regarding this system, the author of the calculated orbit commented at the time of his orbital calculation, "Measures scattered and impossible to interpret" (Couteau 1999). It seems strange then, that Couteau continued with a preliminary orbit calculation in light of that comment. The observational history of this binary is

relatively short, and the techniques used for astrometric measurement consist mostly of visual

micrometry, supplemented by just the three photoelectric phase-grating interferometry

observations and the two recent speckle interferometry observations. The 2008.563 speckle

observation of Gili & Prieur (2012) recorded in the WDS record (see Table 5) does not appear on

the original USNO orbital plot, which was published prior to the work of Gili & Prieur. This

issue has also appeared in two of the other targets of the current work (WDS22357+5413 and

WDS05153+7410). The author has used the 2008.563 speckle observation measurements from

the WDS record to add a representation of this observation to the USNO orbital plot, which falls

nearly on the calculated orbit. The same calculations and additions were performed for the other

USNO orbital plots which did not included the observations of Gili & Prieur.

Table 5. All published astrometric observations of WDS19069+4137:
including the most recent observation data of the current work.

Epoch	θ (°)	ρ (")	Ap.	References	Observation Technique
1984.48	102.9	0.16	0.5	Cou1985a	Ma
1985.744	177	0.07	1	Tok1988	Ig
1988.5255	168.4	0.054	1	Ism1992	Ig
1988.58	91.9	0.13	0.6	Hei1990b	Ma
1990.4432	170.3	0.077	1	Ism1992	Ig
1990.507	77.6	0.213	2	Cou1991a	Mb
1991.6	71.5	0.12	0.6	Gii1994	Ma
1992.553	54.4	0.192	2	Lin1993b	Ma
1992.553	52.2	0.218	2	Doc1993f	Ma
1992.556	60.1	0.178	2	Cou1993d	Ma
1997.714	33	0.2	0.7	Cou2002	Ma
2008.563	348.1	0.211	0.7	Gii2012	S
2013.7967	**325.49**	**0.225**	**2.1**	**Wallace2015**	**S**

The position angle and separation values obtained using the phase grating interferometric

technique in 1985.744, 1988.5255, and 1990.4432 are not in good agreement with the visual

observation values made in similar epochs. This leads one to conclude that either the visual

observations are grossly erroneous, or the phase-grating interferometric observations of

Tokovinin & Ismailov (1988) and Ismailov (1992) are erroneous. This binary is also complicated by the small delta magnitude issue, in that both the secondary and primary are of the same visual magnitude (9.1 according to the WDS and SIMBAD). It is possible that the phase-grating interferometric observations are off due to the primary being mistaken as the secondary and vice versa; however, this author could not reconcile the observations to the visual observations of similar epochs by adjusting the position angles by 180° as is common practice for observations suspected to be confounded by the small Δ mag. issue. The authors have indicated in their work a very large uncertainty regarding the 1985.744 observation, with an error in measured separation larger than 0.02″ (Tokovinin & Ismailov 1988). Similar uncertainty is associated with the measured separation of the 1988.5255 observation, however no observational notes regarding any of the three specific outlying observations can be found within the authors' published works. Thus, it is this author's opinion that these three apparent outlying measurements should be ignored based on the associated uncertainties and the rarity related to use of the photoelectric phase-grating interferometric observational technique, possibly indicating that astrometrists find the technique to harbor too much uncertainty. In support of this conjecture, it can be noted that 18 out of 172, or ~10.5% of the observations of Tokovinin & Ismailov (1988) from 1985-1986 are associated with large uncertainties.

Whichever the case, the error with either group seems to be consistent across the two groups of observations based on the distribution of group population. Moreover, both the visual and interferometric measurement groups could form reasonable arcs with the author's new speckle observation of 2013.7967 and the speckle observation from 2008.563; but it appears a better fit to the data would result if the three phase-grating interferometric observations were ignored. It is not clear from the work of Couteau (1999) if the three phase-grating measurements

60

were considered or ignored at the time of orbit calculation. Whether or not the three

photoelectric phase-grating interferometric observations can be ignored must be determined in

order for this system to be properly understood. Contact with the authors of these three outlying

observations should be initiated, but was not done so prior to the publishing of this work due to

time constraints. The new speckle measurement shows deviation from the calculated orbit, but

perhaps the new speckle measurement would agree more with an orbit calculated using primarily

the interferometric measurements, de-weighting the visual observations. Although the calculated

orbit does not appear to be accurate, as can be seen by the very large O-C line connecting the

new speckle observation to the published orbit, it is possible that the new speckle observation is

not accurate when one considers the strong agreement between the 2008.563 speckle

observations and the published orbit. To resolve this case, future speckle observations will need

to be made. Future observations should confirm whether the author's observation accurately

indicates a deviation from the calculated orbit, and perhaps indicate if a separate orbit calculation

attempt should be made using primarily the interferometric measurements. This system is likely

a true binary as Keplerian motion is evident in all possible interpretations of the system based on

the observational record, however many possible orbital solutions still exist.
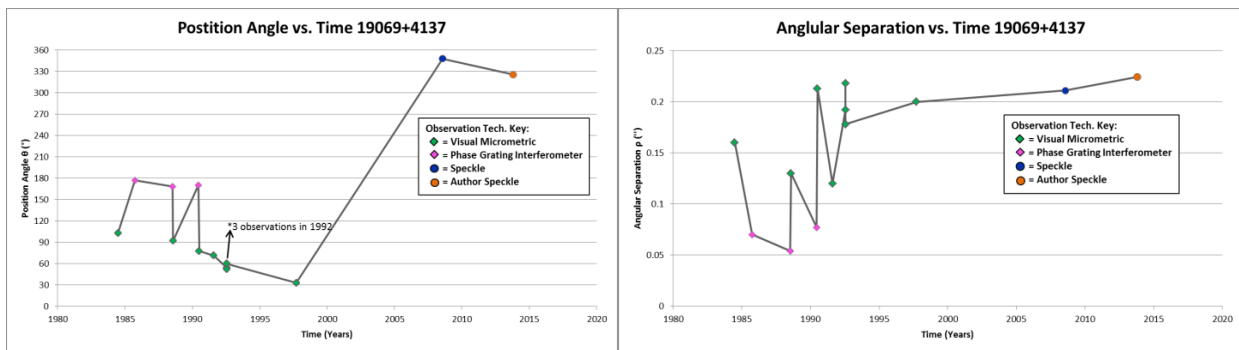
Fig. 24 – Data plots of WDS19069+4137: (Left) Plot of position angle vs. time, (Right) plot of angular separation vs. time for WDS19069+4137.
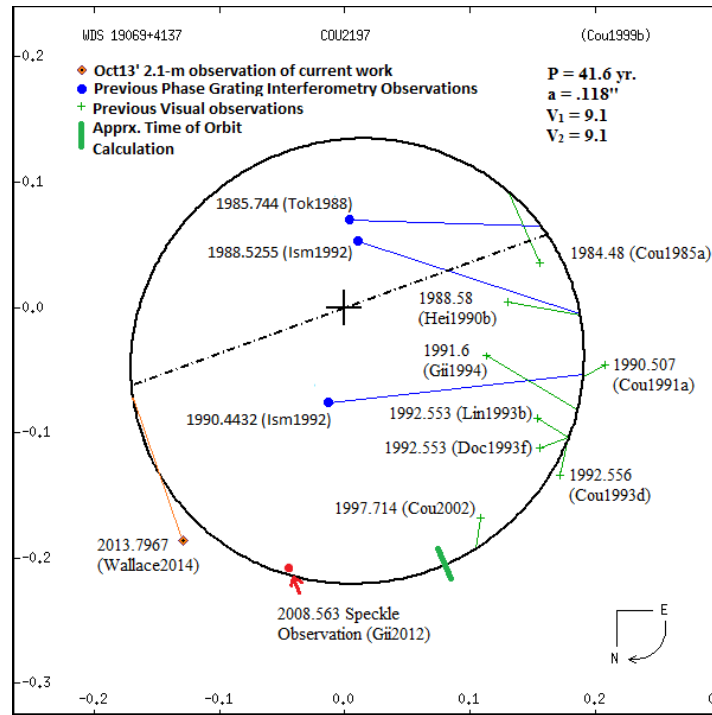
Fig. 25 – Updated USNO orbital plot of WDS19069+4137. Three IG observations (circles) differ drastically from the published orbit and visual observations. The new speckle observation (diamond) indicates nearly a 180° secondary θ translation since the initial visual observation. Orbit appears to be opening. The published orbit (bold) period and semi-major axis are likely too short.

WDS22357+5413

The new speckle observation for WDS22357+5413 agrees well with the preceding three speckle observations of Hartkopf & Mason (2009) and Gili & Prieur (2012) (originally unplotted – the author has calculated position and updated USNO plot with this speckle measure, which appears in the cluster of three speckle observations preceding the new observation of the current work). These speckle observations, made after the premature orbit of 109.49 years (see Fig. 26) was published by Mason & Hartkopf (2001), along with the new observation indicate that the assumed double star WDS22357+5413 is most likely an optical pair; however there is still an outside chance that this system could be a binary. Mason (private communication, 2104) has commented that unless large errors are attributed to the measures, some curvature is apparent, indicating a physical pair. Multiple quadrant adjustments have apparently been applied throughout the data set (1953.7-1964.81, 1995.77, 1996.53, and 1996.7).

Table 6. All published astrometric observations of WDS22357+5413: including the most recent observation data of the current work. Note: 7 WDS observations omitted due to incomplete astrometric data.

Epoch	θ (°)	ρ (")	Ap.	References	Observation Technique
1953.7	167.9	0.39	0.9	Mlr1954a	Mc l
1957.89	170.1	0.39	0.4	Cou1958c	Ma
1960.94	164.8	0.32	0.4	Cou1962a	Ma
1964.81	172.3	0.43	0.3	Hei1967b	Ma
1983.81	3.8	0.15	0.5	Mlr1984	Ma
1983.88	34	0.16	0.5	Mlr1984	Ma
1995.7705	10.6	0.107	2.5	Hrt1997	Sc
1996.5321	9.8	0.119	2.5	Hrt2000a	Sc
1996.6962	9.3	0.126	2.5	Hrt2000a	Sc
2006.5616	178.8	0.243	2.5	Hrt2009	Su
2007.7985	180.1	0.249	2.5	Hrt2009	Su
2008.639	180.3	0.254	0.7	Gii2012	S
2013.7967	**177.04**	**0.306**	**2.1**	**Wallace2015**	**S**

Through investigation of the 1983.81 and 1983.88 observations of Muller (1984), the author has discovered that there is a chance Muller mistakenly observed WDS22342+5405 (also known as ADS16073 and A1468). A1468 appears very close to WDS22357+5413, and Muller himself admits that he has no notes regarding his 1983.81 and .88 observations, and that observers would often confuse the two similar magnitude pairs. Despite lacking observation notes regarding a system that is often mistaken as A1468, Muller (1984) writes that he is certain he observed WDS22357+5413. Unfortunately, personal certainty may not be good enough in the case of this double star. If the two visual observations of 1983 are assumed erroneous, which cannot be ruled out as there exists no record other than the measurements themselves and Muller's personal certainty, then a linear trend to the data emerges (see Fig. 26 and 27). No proper motion data exist for the secondary, which would provide useful information regarding

a possible difference in proper motion between the components and add further evidence against

binarity.
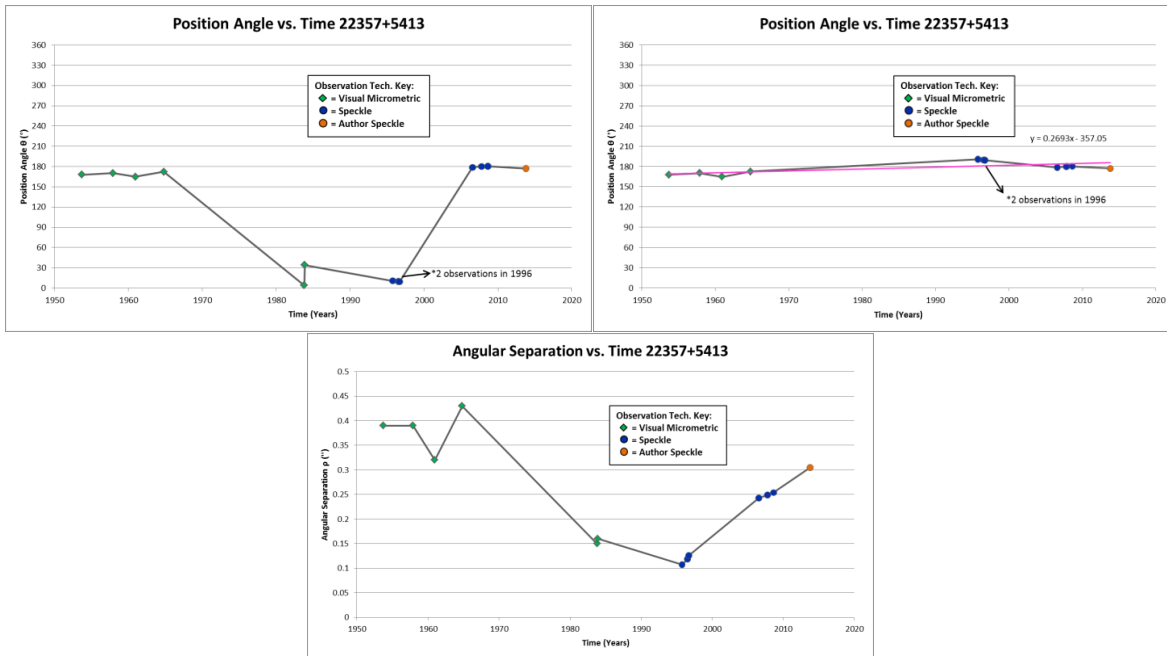
Fig. 26 – Data plots of WDS22357+5413: (Top Left) Plot of position angle vs. time, (top right) linear fit to data emerges if observations from 1983 are ignored and (bottom) plot of angular separation vs. time for WDS22357+5413.
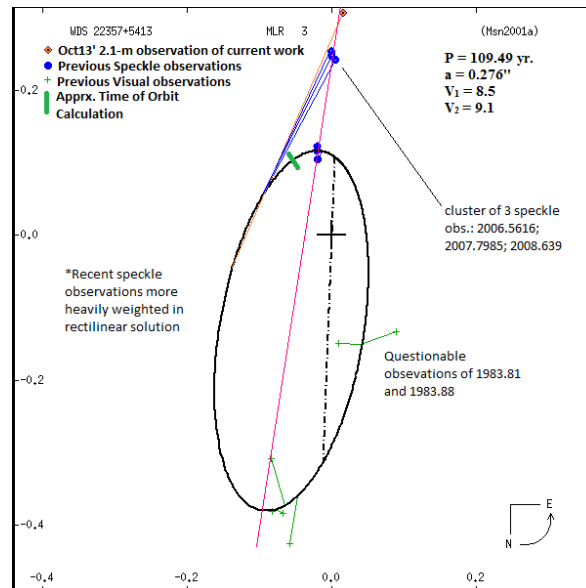
Fig. 27 – Updated USNO orbital plot of WDS22357+5413. Original plot updated with new speckle measurement of the current work and previously unplotted speckle observation from 2008.639, as well as linear fit line to data. Linear fit assumes 1983.81 and .88 are erroneous. The previous speckle observations (circles) have deviated significantly from published orbit (bold). The new speckle observation (diamond) indicates a continuation in linear trend. Binarity is unlikely, but further observations of this system will be needed for confirmation of nature.

WDS02231+7021

The new speckle observation for WDS02231+7021 agrees well with the preceding speckle observations of Mason et al. (2011) and Prieur et al. (2012). When all observations of WDS02231+7021 (see Table 7) are taken into account, it appears that a linear fit can more appropriately describe this system, which suggests an optical pair rather than a true binary. The author has calculated rectilinear solutions based on position angle and separation data for this target, which support this idea, shown below in Fig. 28. The prematurely published orbit of Pavlovic & Todorovic (2005) was computed prior to the most recent speckle observations, including that of the current work.

By the year of the published orbit in 2005, the recorded observations were likely concluded to represent a small portion of the proposed nearly edge-on orbit. It is not clear whether Pavlovic & Todorovic had considered the possibility of WDS02231+7021 being an optical double. The orbit produced very large differences between calculated dynamical parallax and Hipparcos measured parallax typically held as quite accurate, which Pavlovic & Todorovic (2005) accounted for as follows:

> *Our (orbital) elements provide a better fit to the observations; however the obtained dynamical parallax (15.46 mas) is several times that of (pre-updated) Hipparcos (3.39 mas). This can be accounted for by the fact that the measurements cover a short orbit arc (only 15°) and, therefore, the orbital elements are determined with large errors. The discrepancy between π_{dyn} and π_{HIP} is due to the large errors of the values of period and semi-major axis.*

If this system is not a system viewed edge-on, but an optical pair as the recent measurements suggest, then the previous assumption for the parallax discrepancy is

incorrect, and thus so are the calculated masses of these stars: $M_A = 1.079$, $M_B = 1.026$ (masses in units of solar mass).

Table 7. All published astrometric observations of WDS02231+7021: including the most recent observation data of the current work.

Epoch	θ (°)	ρ (")	Ap.	References	Observation Technique
1972.66	162.4	0.48	0.7	Mlr1973a	Ma
1973.76	160	0.61	0.5	Mlr1978b	Ma
1976.51	161.7	0.7	0.5	Mlr1978b	Ma
1979.88	157.6	0.59	0.6	Hei1980a	Ma
1982.22	157	0.68	0.5	Mlr1984	Ma
1983.0663	154.2	0.584	3.8	McA1987b	Sc P
1983.7107	154.1	0.585	3.8	McA1987b	Sc P
1984.9967	153.9	0.611	3.8	McA1987b	Sc P
1985.8541	153.5	0.602	3.8	McA1987b	Sc P
1988.76	157.3	0.75	0.5	Mlr1990	Ma
1991.25	150.2	0.621	0.3	Fab2000a	Hh
1991.64	151.6	0.61	0.3	TYC2002	Ht
1991.9017	149.5	0.625	0.3	Hrt1994	Sc
1992.47	151.5	0.6	0.5	Mlr1993	Ma
1994.99	146.3	0.68	0.6	Hei1996a	Ma
1999.7286	145.3	0.659	1.5	Doc2001c	S
1999.745	144.7	0.62	1.5	Lin2000a	Mb
1999.745	147.1	0.64	1.5	Pri2000a	Mb
2000.98	147.9	0.64	0.3	Alz2003b	Mb
2001.9882	147.7	0.56	0.7	WSI2002	Su
2005.111	142	0.656	1	Sca2007a	S
2007.6022	140.5	0.674	3.8	Msn2011d	Su
2010.053	140.1	0.651	1	Pru2012	S
2013.8104	139.03	0.684	2.1	Wallace2015	S

Currently, no data exist regarding radial velocity or proper motion of the secondary component, which is unfortunate as such data would likely add much clarity to the case of this double star. According to the SIMBAD astronomical database, the radial velocity for the primary is +7.40 km/s (±2.1), the proper motion in RA/Dec is +24.36/-8.41 mas (±1.35/1.49), and the most up to date Hipparcos parallax is 4.64 mas (±1.36). Based on the entire

observational record including the most recent speckle observations, it is unlikely this target is

actually a physical binary.
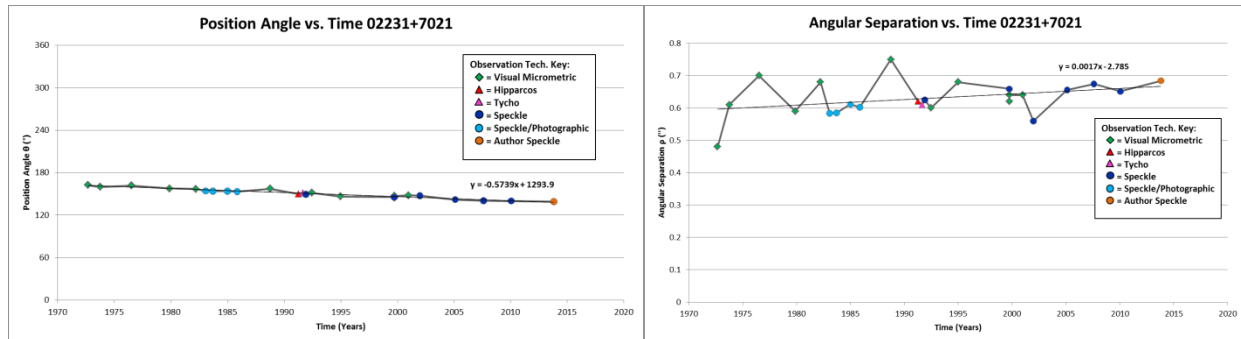
Fig. 28 – Data plots of WDS02231+7021: (Left) Plot of position angle vs. time, (Right) plot of angular separation vs. time for WDS22357+5413. As the data seems to indicate an optical double, linear trend lines and equations have been added to each plot.
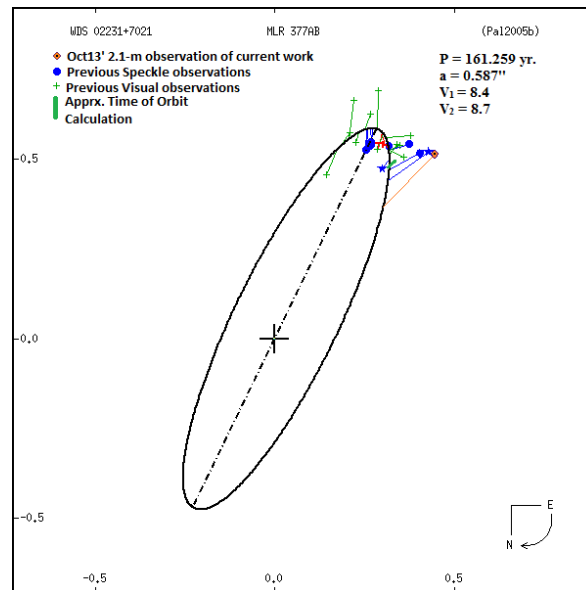
Fig. 29 – Updated USNO orbital plot of WDS02231+7021. The previous speckle observations (circles/stars), are indicating a deviation from published orbit (bold) in a linear manner. The new speckle observation (diamond) agrees with this trend.

A very long period binary, one in which only a small fraction of the orbit has been

observed thus far cannot be completely ruled out. Likewise, a system whose orbit is nearly edge-

on relative to our line of sight cannot yet be undoubtedly ruled out. Such systems would, given

the observed change in position angle and separation over time, exhibit a linear movement

pattern similar to that shown by the observational record. Romero (private communication,

67

2014) has performed an astrophysical study of this system, and has tentatively concluded a 38% maximum probability of binarity based on the dynamic parameters used in Monte Carlo simulations. For certain, the latest speckle observation (shown below in Fig. 29 as the diamond) clearly shows continued deviation from the most recently calculated orbit of 161.259 years, and thus this orbit would be a prime candidate for revision. An orbit should not be reattempted for this system until future observations either confirm or rule out binarity.

WDS04505+0103

The new speckle observation of WDS04505+0103 agrees with the two preceding speckle observations of Mason et al. (2011) and Tokovinin et al. (2010). Recent speckle observations, including that of the author, indicate a deviation from the previously published orbit of 158.4 years computed by Scardia (2003), but offer good evidence of binarity as they exhibit characteristic curves of rectilinear coordinates X & Y vs time. Recent speckle observations indicate an opening of the orbit suggesting that the calculated orbital period and semi-major axis are likely too short. No proper motion or radial velocity data is given for the secondary. This data could prove useful if common proper motion and radial velocities for the components could be shown. Quadrant ambiguity does not seem to have been an issue in the observational history of this system.

Table 8. All published astrometric observations of WDS04505+0103: including the most recent observation data of the current work.

Epoch	θ (°)	ρ (")	Ap.	References	Observation Technique
1913.71	84	0.26	0.9	A__1914a	Ma
1921.72	74.7	0.27	0.9	A__1932a	Ma
1930.99	58.4	0.24	0.9	A__1933d	Ma
1937.84	48.8	0.17	0.6	Vou1947b	Ma
1961.94	334.4	0.12	0.9	B__1962d	Ma

Table 8 cont.

1963.107	319.3	0.26	0.7	Wor1971	Ma
1966.88	308.7	0.1	1.5	Wor1972a	Mb
1981.93	243.3	0.12	0.6	Hei1983a	Ma
1989.9332	88	0.239	4	Hrt1996b	Sc
1990.9216	84.1	0.24	4	Hrt1996b	Sc
1990.9242	85.2	0.243	4	Hrt1996b	Sc
1993.0924	83.4	0.248	4	Hrt1996b	Sc
2008.7703	252.4	0.2917	4.1	Tok2010	S
2010.0653	**252.3**	**0.294**	**3.8**	**Msn2011d**	**Su**
2013.8022	**249.83**	**0.298**	**2.1**	**Wallace2014**	**S**
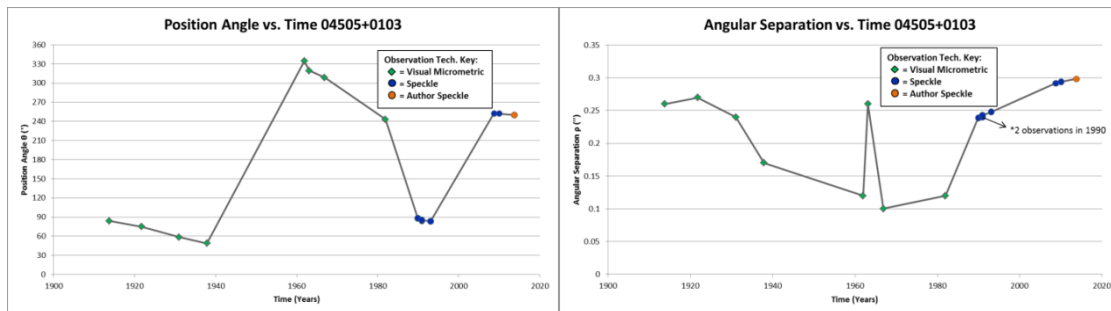
Fig. 30 – Data plots of WDS04505+0103: (Right) Plot of position angle vs. time, (Left) plot of angular separation vs. time for WDS04505+0103.
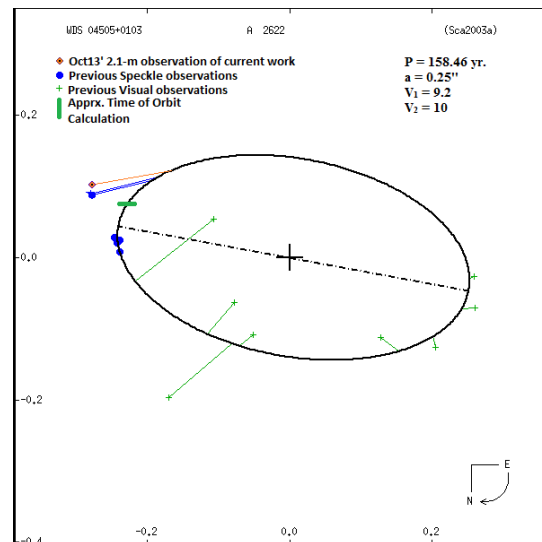
Fig. 31 – Updated USNO orbital plot of WDS04505+0103. Recent speckle observations (circles/star) indicate deviation from published orbit (bold). The new speckle observation (diamond) shows agreement with previous speckle observations and deviation from published orbit, indicating the need for orbital revision.

69

WDS05153+4710

The new speckle observation for WDS05153+4710 demonstrates deviation from the previously published orbit of 513.48 years computed by Zirm (2008) suggesting the need for orbit revision. The 2008.066 speckle observation was not found originally on the USNO orbital plot, but the author has calculated its position and updated the orbital plot with this measurement (see Fig. 33). The deviation of the two recent speckle observations suggest that the computed orbit for this system is too large. The 1999.8371 USNO speckle observation (Mason et al. 2001b) and the nearby 2003.99 visual observation (Alzner 2005) seem to be outliers when compared with observational history of this system. These observations could not be reconciled to this system by the author of this investigation through consideration of quadrant ambiguity.

Table 9. All published astrometric observations of WDS05153+4710: including the most recent observation data of the current work.

| Epoch	θ (°)	ρ (")	Ap.	References	Observation Technique
1905.82	349.2	0.45	0.9	A__1906a	Ma
1916.66	353.6	0.39	0.9	A__1929a	Ma
1919.71	1.2	0.45	0.9	A__1929a	Ma
1933.89	6.8	0.47	0.9	A__1937a	Ma
1943.92	19.9	0.38	1	VBs1954	Ma
1951.08	29.9	0.33	2.1	VBs1954	Mb
1965.99	43	0.33	0.4	Cou1967b	Ma
1969.53	29.3	0.37	2.1	VBs1974	Mb
1970.98	58.6	0.26	0.7	Wor1978	Ma
1991.25	80	0.358	0.3	HIP1997a	Hh
1991.56	73.6	0.4	0.3	TYC2002	Ht
1999.8317	143.1	0.736	2.1	Msn2001	Su
2003.723	91.4	0.4	0.5	Slm2005	C
2003.99	319.4	0.75	0.3	Alz2005b	Mb
2008.066	97.6	0.368	0.7	Gii2012	S
2013.8022	**106.31**	**0.390**	**2.1**	**Wallace2014**	**S**

The author has communicated directly to Mason and Alzner (private communication, 2015) and both Mason and Alzner conclude their measures to be erroneous. Upon investigation of his own observations, Mason has shown that the 1999.8371 measure was actually of object STT 98 (Shioya-Taniguchi-Trentham 2001), and Alzner (2005) comments, *in 2004.94, I could not confirm my measurement from 2003.99*. Alzner's comment, along with recent discussion with this author regarding the uncertainty of the 2003.99 measurement strengthens the conjecture that this measurement is also erroneous. It is also unclear as to whether or not Zirm (2008) considered these observations in his preliminary orbit calculation. Future observations will be needed to confirm deviation from the published orbit. When the 1999.8371 and 2003.99 outliers are ignored, then the observational record demonstrates Keplerian motion that suggests binarity, however it appears the calculated orbit is not a good fit considering recent observations.
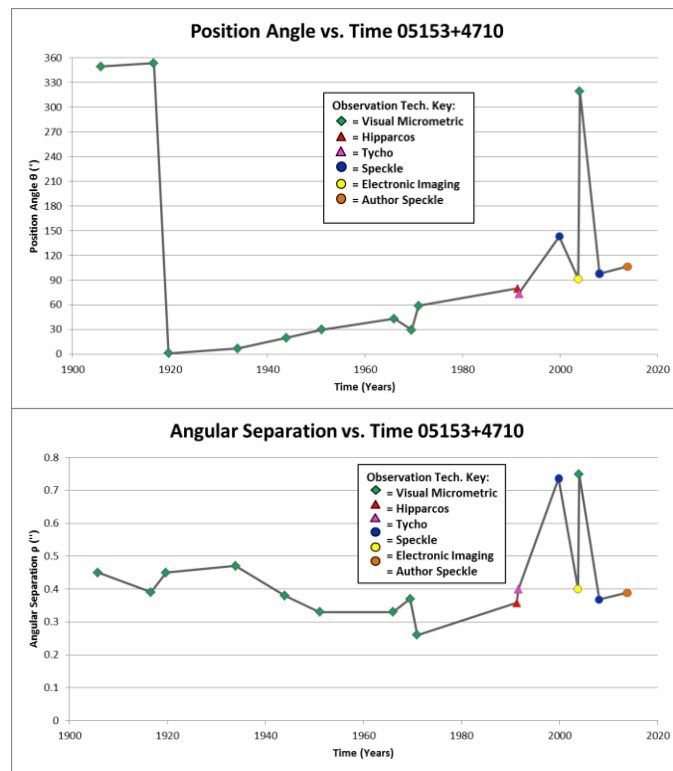

Fig. 32 – Data plots of WDS05153+4710: (Top) Plot of position angle vs. time, (bottom) plot of angular separation vs. time for WDS05153+4710.
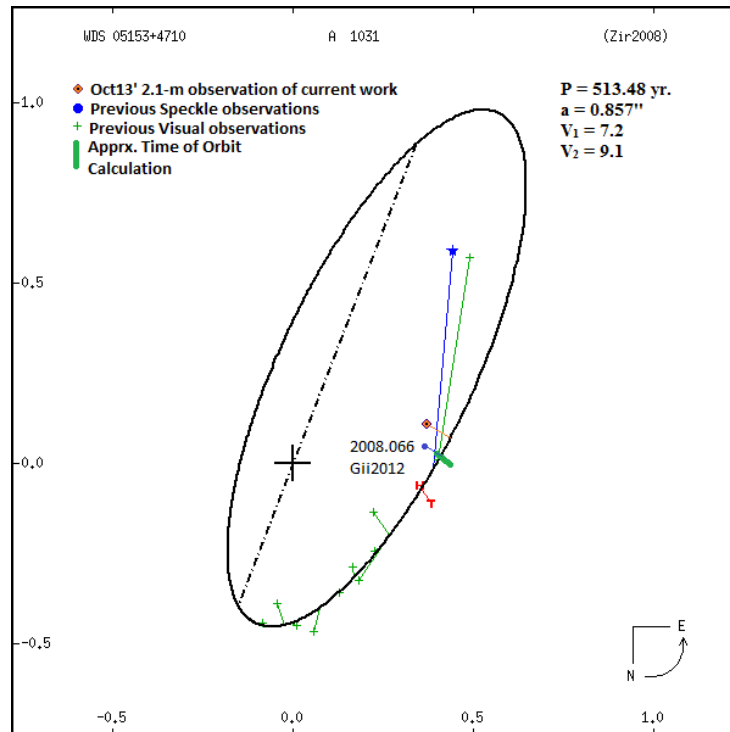
Fig. 33 – Updated USNO orbital plot of WDS05153+4710. The previous USNO speckle observation (blue star), and nearby visual observation (green plus sign) deviated significantly from previous visual observations and published orbit (bold). The new speckle observation (diamond) has deviated from published orbit, possibly indicating the need for orbital revision.

WDS06256+2227

The new speckle observation for WDS06256+2227 agrees well with the previous speckle observation of Orlov et al. (2009). These lone speckle observations agree generally with the observed deviation from the published orbit of 360.3 years computed by Scardia (2001). Interestingly, this orbit was described after publishing of the Hipparcos and Tycho observations, which also do not agree with the computed orbit. A time-lapse of approximately 50 years occurred where no observations of this system were made – a truly unfortunate situation, as it appears that during this time the secondary passed through the critical periastron point. However, one must ask if the apparent 180° translation of the secondary in its orbit over a 50 year period is consistent with the proposed total orbital period of 360.0 years. Certainly the secondary would pass through periastron and surrounding orbital points much faster than

72

opposite points on the orbit near apastron according to Kepler's laws, but would 50 years be enough time to account for this? The large amount of orbit not covered by observations also tempts one to conclude a possible quadrant ambiguity issue for this system early on its observational record, as it appears that linearity would be evident if the early visual observations of position angle were adjusted by 180°. Adjusting the position angles of the early observations would place the initial eight micrometric observations relatively in-line with the measurements starting in 1950. The author has calculated the adjusted positions for the eight early visual observations, which are shown as brown crosses below in Fig. 35 (right).

A good linear fit to the observational record with adjustments to early position angle data provides some evidence for the system being an optical double rather than a true binary. The plot of position angle vs. time in Fig. 34 has also been shown with the early visual measurements adjusted, and a rectilinear solution has been provided. Although the linear solutions seem promising, one must also consider that the difference in magnitude between the primary (+7.3) and secondary (+9.4) is not very small compared to many other double stars. Indeed, based on the difference in visual magnitude, the primary would appear 6.85 times brighter than the secondary, and it would seem to be difficult to mistake the two in visual observations. Moreover, the WDS catalog and SIMBAD indicate common proper motion for the secondary and primary of RA 9.63 mas/yr (±1.05) and Dec -15.54 mas/yr(±0.69), which is further evidence for binarity (van Leeuwen 2007). Thus, there appears to be evidence for the system regarding both binarity and being an optical double. If future observations begin to indicate an arc back towards the original unadjusted positions, then the system is likely a true binary and the orbit will need to be revised. However, if future observations show continued linear trend then the system will likely be republished as an optical pair.

Table 10. All published astrometric observations of WDS06256+2227: including the most recent observation data of the current work.

Epoch	θ (°)	ρ (")	Ap.	References	Observation Technique
1843.23	312.5	0.78	0.3	Mad1844	Ma
1847.22	302.4	0.91	0.4	Stt1878	Ma
1857.49	243.8	0.4	0.3	Se_1860	Ma
1868.32	311.97	0.7	0.2	D__1870f	Ma
1870.38	314	0.7	0.2	D__1883	Ma
1891.2	324.2	0.45	0.8	StH1901	Ma
1899.5	329.2	0.4	0.9	Hu_1901a	Ma
1900.667	324.8	0.55	0.5	Doo1905a	Ma
1955.8	229.9	0.28	2.1	VBs1960	Mb
1956.16	220	0.32	0.6	Mlr1956a	Mc
1958.03	235.8	0.28	2.1	VBs1960	Mb
1959.15	238.2	0.39	2.1	VBs1960	Mb
1959.151	238.2	0.39	1	VBs1965	Ma
1960.198	242.6	0.41	2.1	VBs1965	Mb
1961.2	232.2	0.34	0.3	Hei1963b	Ma
1961.21	234.5	0.4	0.4	Baz1964	Ma
1961.25	238.2	0.4	0.9	VBs1965	Mb
1961.84	229.4	0.34	0.9	Cou1962b	Mb
1962.18	235.2	0.4	0.3	Hei1963b	Ma
1962.757	232.7	0.32	0.7	Wor1967b	Ma
1962.9	234.4	0.34	0.9	B__1963b	Ma
1966.18	**235.9**	**0.47**	**0.4**	**Baz1967**	**Ma**
1966.307	239.1	0.42	1.5	Wor1971	Mb
1969.2	240	0.44	0.3	Hei1970b	Ma
1975.128	243.3	0.4	0.7	Wor1978	Ma
1980	243.7	0.46	0.6	Hei1983a	Ma
1990.151	255.4	0.63	0.7	Wor1998	Ma
1991.25	250	0.597	0.3	HIP1997a	Hh
1991.81	252.7	0.58	0.3	TYC2002	Ht
1996.21	253.7	0.49	0.4	Alz1998b	Mb
1997.18	255.4	0.6	0.6	Hei1998	Ma
1997.41	251.1	0.48	0.3	Alz1998b	Mb
2004.06	259.1	0.63	0.3	Alz2005b	Mb
2008.11	260.1	0.74	0.3	Alz2008	Mb
2008.8882	256.7	0.72	1	Orl2009	S
2011.05	257	0.736	?	OCC2012b	O
2013.7967	**256.06**	**0.738**	**2.1**	**Wallace2014**	**S**
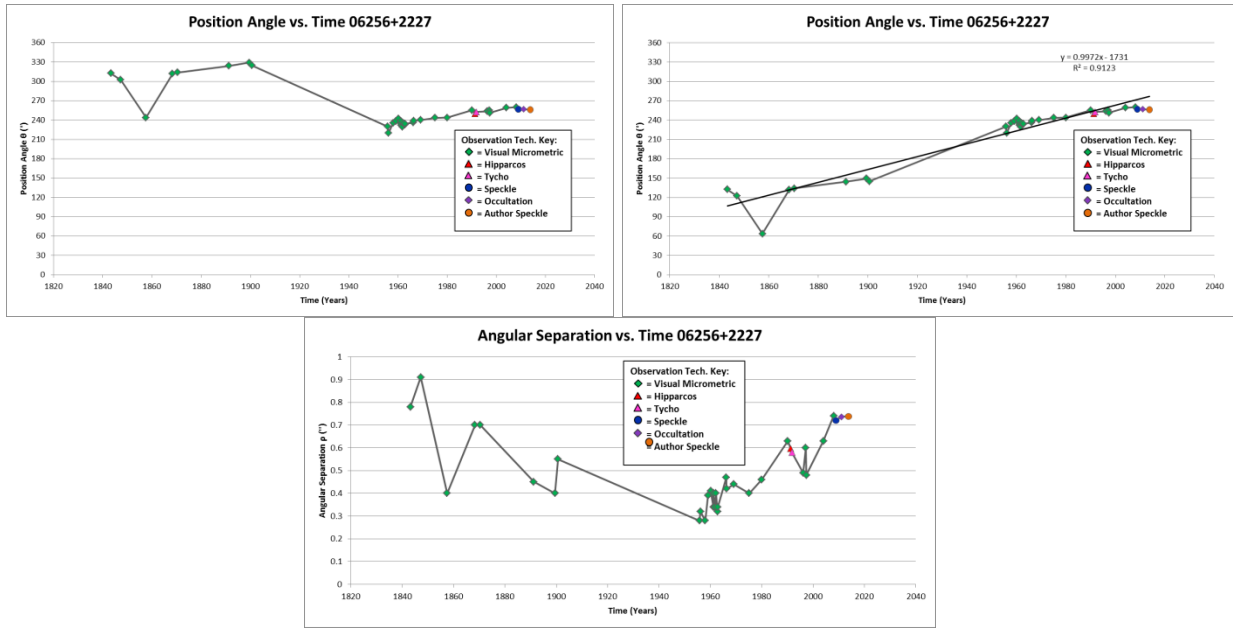
Fig. 34 – Data plots of WDS06256+2227: (Top Left) PA vs. time, (Right) the same plot but with 180° adjustment to PA of early visual obs. made, (Bottom) separation vs. time for WDS06526+2227.
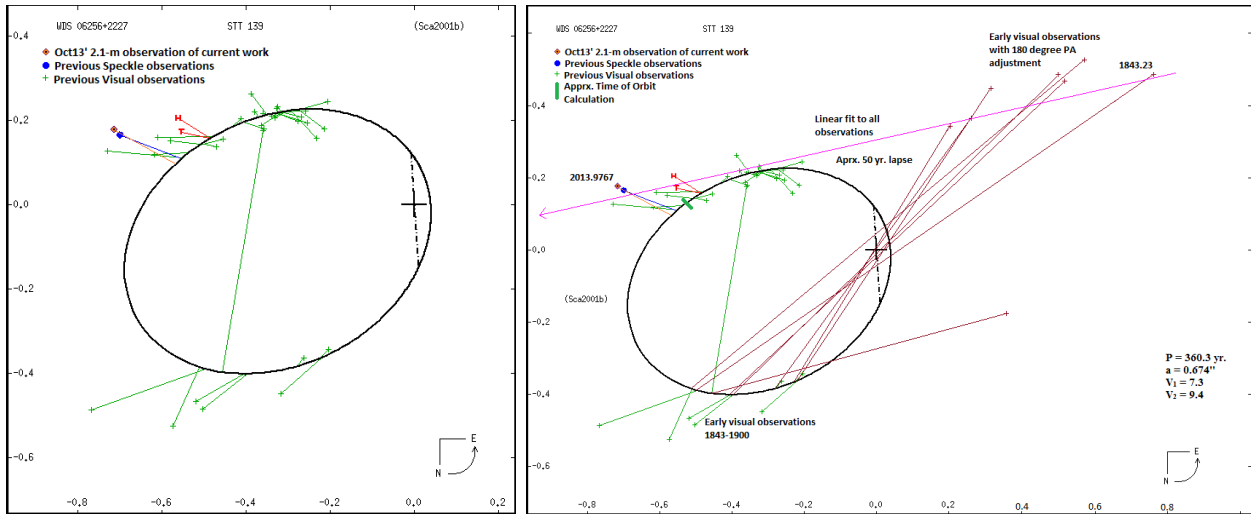
Fig. 35 – Updated USNO orbital plot of WDS06256+2227. (Left) The previous speckle observation (blue circle), recent visual observations (green plus signs) and Hipparcos & Tycho observations (red H & T) indicate deviation from published orbit (bold). New speckle observation (diamond) shows agreement with indicated deviation from published orbit. (Right) Brown crosses represent 180° PA flip of early visual observations. Pink line indicates linear best fit, with recent observations more heavily weighted.

Conclusions

The primary aim of this work has been to obtain, via speckle interferometry on the 2.1-meter KPNO telescope, quality astrometric information of six purposely selected close visual

double stars whose recent astrometric data demonstrate deviation from published orbits such that one additional quality speckle interferometric observation, might resolve the deviation as anomalous or as a continued trend indicating the need for orbital revision or reconsideration of binarity. Complementary to the main goal, the effort demonstrated the applicability, integration ability, and utilization of relatively low-cost portable speckle camera systems on large telescopes, as well as the value of student participation and contribution within the realm of a large-scale observing run at a major observatory and the resulting peer reviewed scientific works that follow. The effort in its entirety demonstrates a multi-edged solution to various problems within the double star science field, such as the lack of quality ground-based close visual double star follow-up work due to the relatively low number of observers and programs, the highly competitive nature of obtaining time on large telescopes, and the flood of new double star data from recent space-based surveying projects.

As a result of this investigation, several conclusions regarding the specific target double stars have been made. In the case of WDS02231+7021, the author's speckle observation has provided evidence against binarity and the latest calculated orbit of Pavlovic & Todorovic (2005). Rectilinear solutions have been provided in further support of the conclusion of non-binarity for this system. Radial velocity and proper motion measurements of the secondary component would add much to the understanding of this pair, but it is likely that future speckle observations will indicate continued linear trend away from the prematurely published orbit.

WDS19069+4137 is likely a true binary, as Keplerian motion is evident from the observational record including the observation of the current work; however the calculated orbit, likely being too short, will undoubtedly need revisions based on future speckle observations. The short observational history, coupled with the three outlying photoelectric phase-grating

76

interferometric observations make this system difficult to interpret at the moment. It must be determined why the phase-grating observations differ so much from the visual observations made across very similar epochs, and also if they can be ignored or not.

The conclusion that WDS06256+2227 may actually be an optical double rather than a physical pair is supported if one assumes the eight initial visual observations spanning 1843-1900 fell prey to the small delta magnitude issue, and that for these observations the position angle should be adjusted by 180°. However, the fact that the components do not exhibit a small difference in magnitude does not support the idea that previous visual observers would mistake the 6.85 times brighter primary for the secondary. Future observations will either demonstrate continued linear trend or curvature back towards the original unadjusted early visual positions.

All of the WDS04505+0103 observational data together demonstrate curvature regarding position angle and separation, thus the system is likely a binary. However, the new speckle observation demonstrates continuation in the trend of deviation from the published orbit indicating the need for orbital revision. The calculated orbital period and semi-major axis for this system are likely too short.

WDS22357+5413 is likely an optical double star, as the new speckle observation seems to continue the recent linear trend exhibited by all the speckle data for this system. Several 180° position angle adjustments are evident in the observational record. The components of WDS22357+5413 differ by only .6 in magnitude, corresponding to a brightness difference of only 1.73, thus it is conceivable that visual observers in the past could have mistaken the originally identified primary for the secondary. According to Muller (1984), the observations of 1983.81 and .88 that fall in the middle of the observational record for WDS22357+5413 are not

77

of nearby A1468; however if Muller's 1983 observations are ignored under the assumption of error, then a clear linear fit to the data emerges.

Currently, WDS05153+4710 data include two outlying measurements – a USNO speckle measurement (1999.8371) and one visual measurement (2003.99) from just before the published orbit was calculated. These measures could not be reconciled with the pervious observations or calculated orbit, and were shown to be erroneous. As a result of this investigation, these measures will be removed from the record of WDS05153+4710. It is unlikely that these outlying measurements were included in the orbit computation. Regardless, the recent speckle observations including that of the current work show a deviation from the calculated orbit such that an orbit with shorter period and semi-major axis is likely. Keplerian motion appears evident for this system, thus binarity is supported.

The investigated targets are typical of WDS problematic binaries, that is, those close visual binaries whose data show an emerging disagreement between recent speckle observations and the previously calculated orbits, and whose orbits are preliminary and tentative in nature because they are based on relatively sparse observational records dominated by older visual observations. The common theme of previously published orbits not agreeing with recent speckle observations encountered in this investigation can be understood if one realizes that the premature orbits published for these double stars usually represent best-fit solutions to the observational records, which are primarily composed of older and less reliable visual micrometric observations. While visual observations of more widely spaced stars can be highly accurate, visual observations of very closely separated stars, like the six targets investigated here, are subjective at best, and suffer greatly in the cases of double stars with very small differences in visual magnitudes, often resulting in a 180° quadrant ambiguity as successive observers

mistake the originally identified secondary for the primary or vice versa. This can lead to visual

technique dominated observational records of close visual double stars with very large

differences among astrometric measurements, which in turn would negatively influence the

calculated orbits causing the observed disagreement with recent high quality speckle

observations. Such speckle observations of close visual double stars are more accurate and

precise than visual measurements on average by an order of magnitude, and thus it may be that

the majority of close visual double star cases similar to the six targets of the current work will

need follow-up work and revisions of orbits based mainly (largest weights) on recent speckle

observations. Assigning less significant weights to questionable visual observations can help to

better inform the orbit, however in double star cases where the observational record includes

only a handful of previous visual observations which cover a small fraction of the proposed

binary orbit, the computed orbit will likely be a poor description unable to accurately predict

future positions of the components. In these cases, deviation of recent speckle observations from

very tentative orbits computed based on little and uncertain data seems inevitable.

In addition to the targets' poorly descriptive orbits, erroneous observations were apparent

in at least two of the investigated binaries – WDS05153+4710 and WDS19069+4137. Such

measurements may confound many similar problematic binaries throughout the WDS catalog,

and it is important to determine if these observations should be removed from the records or not

by referencing the observer's notes, if any such notes exist, or by contacting the authors directly.

In light of these conclusions and the flood of new double star discoveries pouring in from space-

based observing missions and new optical interferometer projects, the application of speckle

interferometry follow-up work on large telescopes, and investigations of problematic binaries

like that of this work will become ever more important. From this effort, the most up to date

calibration values have been obtained for the observations of the KPNO I speckle interferometry run, which will serve as the comparative standard in future calibration refinements, and in turn estimations of accuracy. There are currently a great many more problematic binaries within the WDS for which investigations like those carried out in this effort are needed. Future work regarding methods used in this investigation include the application of portable speckle interferometry systems to larger ground-based telescopes to obtain new astrometric data of ever more close visual double stars. Automation or at least semi-automation of the speckle interferometric method to observe close visual double stars is also desirable, and will likely be developed in the future. Better constraints on duplicity and multiplicity, as well as stellar mass distribution regarding the observable galactic stellar population will result from continued double star observation and follow-up work. Finally, obtainment of high angular resolution images of distant star systems via the application of speckle interferometry on extremely large telescopes, such as the planned Thirty Meter Telescope (TMT), could conceivably make the resolution of large exoplanets from the ground commonplace.

APPENDICES

Table 11: Summary of internal precision estimate data. All position angle and separation values given in image frame pixels.

WDS	μ $\theta_{Obs.}$ (°$_{IF}$)	σ $\theta_{Obs.}$ (°$_{IF}$)	$\sigma_{\bar{x}}$ $\theta_{Obs.}$ (°$_{IF}$)	Within Nights σ $\theta_{Obs.}$ (°$_{IF}$)	Between Nights σ $\theta_{Obs.}$ (°$_{IF}$)	μ $\rho_{Obs.}$ (Pixels$_{IF}$)	σ $\rho_{Obs.}$ (Pixels$_{IF}$)	$\sigma_{\bar{x}}$ $\rho_{Obs.}$ (Pixels$_{IF}$)	Within Nights σ $\rho_{Obs.}$ (Pixels$_{IF}$)	Between Nights σ $\rho_{Obs.}$ (Pixels$_{IF}$)
03122+3713	114.3077	0.0202	0.0072	0.0089	0.0191	242.2361	0.3750	0.0830	0.3750	0.3922
01532+1526	248.9848	0.0288	0.0139	0.0152	0.0277	96.0698	0.0953	0.0287	0.0953	0.1036
23595+3343	327.5824	0.0197	0.0063	0.0115	0.0167	198.8800	0.2287	0.0900	0.2287	0.2109
03362+4220	332.9710	0.0353	0.0146	0.0128	0.0359	62.2580	0.1266	0.0402	0.0127	0.1260
04041+3931	43.6908	0.0322	0.0158	0.0164	0.0316	128.9400	0.0778	0.0318	0.0778	0.0786
	Average	**0.0272**	**0.0116**	**0.0130**	**0.0262**	**Average**	**0.1807**	**0.0547**	**0.1579**	**0.1822**
						arcseconds	**0.0021**	**0.0006**	**0.0018**	**0.0021**

Table 12. Summary of accuracy estimate data. All position angle (θ) values given in degrees, and all separation (ρ) values given in arcseconds. Note: mean O-C values representing overall θ and ρ observational accuracy are slightly higher than quoted in chapter 3, as the values below are representative of grand averages.

WDS	μ θO-C (°)	σ θO-C (°)	$\sigma_{\bar{x}}$ θO-C (°)	Within Nights σ θO-C (°)	Between Nights σ θO-C (°)	μ ρO-C (arcsec.)	σ ρO-C (arcsec.)	$\sigma_{\bar{x}}$ ρO-C (arcsec.)	Within Nights σ ρO-C (arcsec.)	Between Nights σ ρO-C (arcsec.)
03122+3713	0.498736	0.020222	0.007230	0.008877	0.019129	0.015770	0.004389	0.001735	0.000971	0.004590
01532+1526	0.562342	0.028756	0.013860	0.015227	0.027721	0.032091	0.001115	0.000606	0.000336	0.001212
23595+3343	0.007244	0.019657	0.006308	0.011463	0.016690	0.015009	0.002677	0.000933	0.001053	0.002468
03362+4220	0.642383	0.035291	0.014637	0.012824	0.035852	0.006197	0.001481	0.000602	0.000470	0.001475
04041+3931	0.425228	0.032237	0.015805	0.016396	0.031609	0.007432	0.000910	0.000460	0.000373	0.000920
Average	0.427187	0.027233	0.011568	0.012957	0.026200	0.015300	0.002114	0.000867	0.000641	0.002133

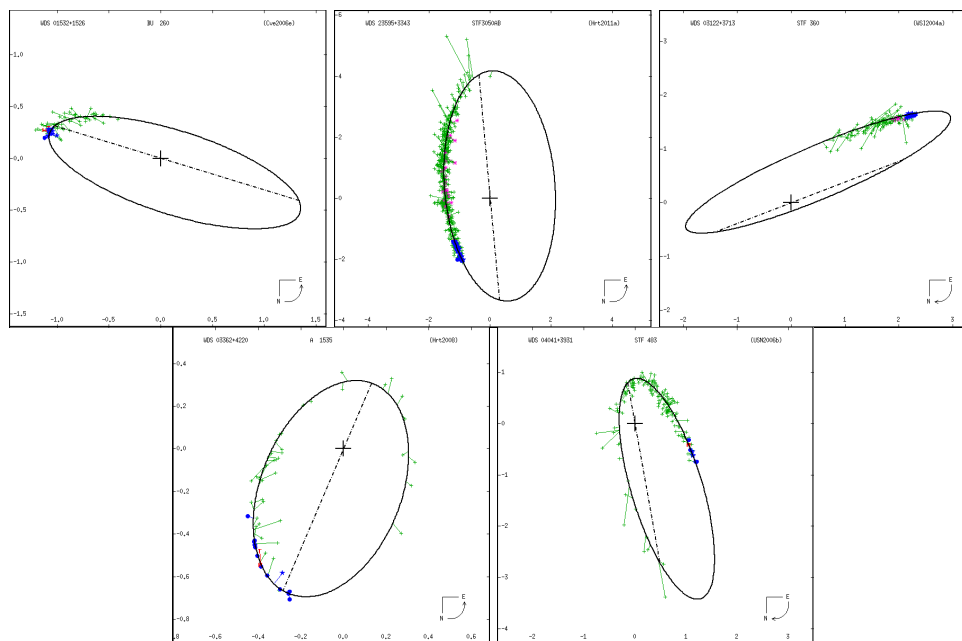**Fig. 36 – The orbits of the five calibration binaries for the Oct. 2013 2.1-metereter speckle run. Most are based on observational records spanning less than half of the described orbit; however for most the data is well-fitting. Reading from top left to bottom right, the calibration binaries and associated USNO orbital grades are: WDS01532+1526 (5), WDS23595+3343 (4), WDS03122+3713 (5), WDS03362+4220 (3), and WDS04041+3931 (4).**
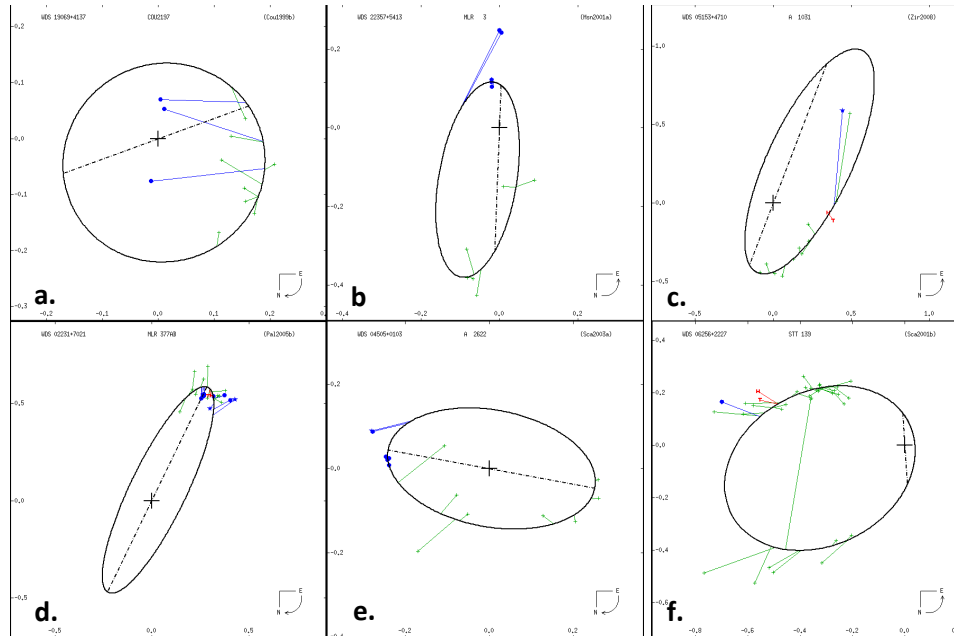
Fig. 37 – USNO orbital plots for the six target binaries. Deviations from computed orbits (bold), indicated by recent observations are obvious. Some observations show trend which could indicate a different orbit than previously calculated (plot d), others seem to indicate the need for reconsideration of binary nature (plot e). Orbital Plots: a.(19069+4137), b.(22357+5413), c.(05153+4710), d.(02234+7021), e.(04505+0103), f.(06256+2227) (USNO 2015c).

Appendix C

Table 13. Published orbital data for the six target binaries from the Sixth Catalog of Orbits of Visual Binary Stars, as well as useful dates and USNO orbit grades. Orbital parameter codes: P (period), a (semi-major axis), i (inclination), Ω (omega), T_0 (time of periastron passage), e (eccentricity), ω (longitude of periastron), EN (equinox of node), E_{last} (date of last observation), # (USNO orbit grade). Uncertainties given where available (USNO 2015c).

WDS	P (yr.)	+/-	a (")	+/-	i (°)	+/-	Ω (°)	+/-	T_0 (yr.)	+/-	e	+/-	ω (°)	+/-	EN	E_{last}	#
19069 +4137	41.6		0.188		160		110		1979.51		0.25		276				5
22357 +5413	109.49		0.276		64.5		177.8		2211.22		0.645		318.9		2000	1996	5
05153 +4710	513.48		0.857		69.8		158.9		1875.32		0.564		133		2000	2004	5
02231 +7021	161.259	83.563	0.587	0.195	104.33	15.43	154.1	21.9	1918.14	13.85	0.115	0.339	199.1	50.6	2000	2001	5
04505 +0103	158.46		0.25		123.8		79.5		1988.44		0.022		163.4		2000	1993	5
06256 +2227	360.3		0.674		56.6		183.8		1929.06		0.894		276.3		2000	1997	5

REFERENCES

Abt, H. A. & Levy, S. G. (1976) Multiplicity Among Solar-Type Stars. Astrophysical Journal Supplement Series, vol. 30, [273-306].

Alzner, A. (2005) Micrometer measurements from 2002.97 to 2004.94. The Webb Society Double Star Section Circulars, No. 13, [6].

Argyle, R. W. (2012) Observing and Measuring Visual Double Stars 2nd Ed. Springer, New York, [5].
    2. Ibid, [71].
    3. Ibid, [vii].
    4. Ibid, [53].
    5. Ibid, [54].
    6. Ibid, [vii].
    7. Ibid, [8-9].
    8. Ibid, [13-15].
    9. Ibid, [5].
    10. Ibid, [71].
    11. Ibid, [5].
    12. Ibid, [85].
    13. Ibid, [106-107].
    14. Ibid, [263].
    15. Ibid, [264].
    16. Ibid, [200].
    17. Ibid, [209].
    18. Ibid, [217].

Buchheim, R. K. (2008) CCD Measurements of Visual Double Stars. The Society for Astronomical Sciences 27th Annual Symposium on Telescope Science. 5/20-22/2008, Big Bear Lake, CA. Published by the Society for Astronomical Sciences, [13]

Couteau, P. (1981) Observing Visual Double Stars. The MIT Press, Cambridge, Massachusetts. [viii].
    2. Ibid, [174].
    3. Ibid, [4].
    4. Ibid, [7].
    5. Ibid, [110].
    6. Ibid, [67].

Couteau, P. (1999) Cat. de 2700 Etoiles Doubles "COU," Obs. de la Cote d'Azur, 3rd ed.

Cutnell, J.D., & Johnson, K.W. (2004) Physics 6th ed.. John Wiley & Sons, Inc. U.S., [821-837].

Dainty, J.C. (1981) Speckle Interferometry in Astronomy. In: Recent advances in observational astronomy. (A82-39606 19-89) Villa Obregon, Mexico, Universidad Nacional Autonoma de Mexico, 1981, p. 95-109; Discussion, [109-111].

Delfosse, X., Beuzit, J.-L., Marchal, L., et al. (2004) Spectroscopically and Spatially Resolving the Components of the Close Binary Stars. ASP Conf. Ser., 318, [166].

Duquennoy, A., & Mayor, M. (1991) Multiplicity Among Solar-Type Stars in the Solar Neighborhood II. Astronomy & Astrophysics. 248, [485-524].

Finsen, W.S. (1964) Interferometer Observation of Binary Stars. Astron. J. Vol. 69, [319-324].

Genet, R.M. (2013a) Portable Speckle Interferometry Camera System. Journal of Astronomical Instrumentation Vol. 2, No. 2.

Genet, R.M. (2013b) Speckle Interferometry and Photometry of Binary Stars. NOAO Observing Proposal.

Genet, R.M. (2014a) Private communication.

Genet, R. M., Gener, R., Rowe, D., Smith, T. C., Teiche, A., Harshaw, R., Wallace, D.B., Weise, E., Wiley, E., Boyce, G., Boyce, P., Branston, D., Chaney, K., Clark, R. K., Estrada, C., Estrada, R., Frey, T., Green, W. L., Haurberg, N., Jones, G., Kenney, J., Loftin, S., McGieson, I., Patel, R., Plummer, J., Ridgely, J., Trueblood, M., Westergren, D. & Wren, P. (2014b) Kitt Peak Speckle Interferometry of Close Visual Binary Stars. The Journal of the American Association of Variable Star Observers, vol. 42, no. 2, [479].

Genet, R. M. & Wallace, D.B. (2015) Precision and Accuracy of Kitt Peak I Speckle Interferometry Observations. In preparation.

Gili, R. & Prieur, J.L. (2012) AN 333, [727].

Gizis, J. E., Reid, I. N., Knapp, G. R., Liebert, J., Kirkpatrick, J. D., Koerner, D. W., & Burgasser, A. J. (2003) Hubble Space Telescope Observations of Binary Very Low Mass Stars and Brown Dwarfs. The Astronomical Journal, 125, [3302-3310].

Halbwachs, J.L., Mayor, M., Udry, S., & Arenou, F. (2003) Multiplicity Among Solar-Type Stars III. Astronomy & Astrophysics, 397, [159-175].

Hartkopf, W.I., McAlister, H.A., & Franz, O.G. (1989) Binary Star Orbits from Speckle Interferometry. II. Combined Visual/Speckle Orbits of 28 Close Systems. The Astronomical Journal, 98:3, [1014-1039].

Hartkopf, W.I., Mason, B.D., & Worley, C.E. (2001a) Sixth Catalog of Orbits of Visual Binary Stars http://www.ad.usno.navy.mil/wds/orb6/orb6.html.

Hartkopf, W.I. & Mason, B.D. (2009) AJ 138, [813].

Heintz, W.D. (1978) Double Stars. D. Reidel Publishing Company, Dordrecht, Holland. [55-59]
      2. Ibid, [vii].
      3. Ibid, [1].
      4. Ibid, [4].
      5. Ibid, [3].
      6. Ibid, [4].
      7. Ibid, [32-33].
      8. Ibid, [59].
      9. Ibid, [25-26].

Heintz, W.D. (1988) The Castor System. Astronomical Society of the Pacific, Publications (ISSN 0004-6280), vol. 100, [834-838].

Henry, T., Monet, D., Shankland, P., Reid, M., van Altena, W., & Zacharias, N. (2009) Astro2010: The Astronomy and Astrophysics Decadal Survey, Science White Paper no. 123. National Academies of Science.

Hoffmann, M.F. (2000) A Search for Binary Stars Using Speckle Interferometry. Senior Research SIMG-503, Center for Imaging Science, Rochester Institute of Technology.

Horch, E. (2006) The Status of Speckle Imaging in Binary Star Research. RevMexAA Vol. 25, [79-82].

Ismailov, R.M. (1992) Interferometric observations of double stars in 1986 1990.   Astron. Astrophys., Suppl. Ser., 96, [375-377].

Jaschek, C. and Gomez, A.E. (1970) The Frequency of Spectroscopic Binaries Publications of the Astronomical Society of the Pacific, Vol. 82, No. 488, [809].

Kaehler, H. (1978) The Vogt-Russell theorem, and new results on an old problem. In: The HR diagram - The 100th anniversary of Henry Norris Russell. IAU Symp. 80 (HR diagram) Dordrecht. ed. A. G. Davis Philipp & D. S. Hayes. D. Reidel Publishing Co. [303-311].

King, B. (2014) See Summer's Best Naked-Eye Double Stars. Sky and Telescope. http://www.skyandtelescope.com/astronomy-news/observing-news/see-summers-best-naked-eye-double-stars-07092014/.

Labeyrie, A. (1970) Attainment of Diffraction Limited Resolution in Large Telescopes by Fourier Analysing Speckle Patterns in Star Images*. Astron. & Astrophys. 6, [85-87].

Lada, C. J. (2006) Stellar Multiplicity and the Initial Mass Function: Most Stars are Single. The Astrophysical Journal, 640, [L63-L66].

Leinert, C., Henry, T., Glindemann, A., & McCarthy Jr., D. W. (1997) A Search for Companions to Nearby Southern M Dwarfs with Near-Infrared Speckle Interferometry. Astronomy & Astrophysics, 325, [159-166].

Mason, B.D. & Hartkopf, W.I. (2001) Inf. Circ. 143.

Mason, B.D, Hartkopf, W.I., Holdenried, E.R., and Rafferty, T.J. (2001b) Speckle interferometry of new and problem Hipparcos binaries. II. Observations obtained in 1998-1999 from McDonald observatory. Astron. J., 121, [3224-3234].

Mason, B.D., and Hartkopf, W.I. (2003) Speckle Interferometry with Small Telescopes. In: The Future of Small Telescopes in the New Millennium. Astrophysics and Space Science Library. 287/8/9. Kluwer Academic Publishers. Springer Netherlands. [129].

Mason, B.D., Hartkopf, W.I., Raghavan, D., Subasavage, J.P., Roberts, L.C., Jr., Turner, N.H., & ten Brummelaar, T.A. (2011) AJ 142, [176].

Mason, B.D., Wycoff, G.L., & Hartkopf, W.I. (2012) The Washington Double Star Catalog, U.S. Naval Observatory: Washington.

Mason, B.D. (2015) Private communication.

Massey, P. & Meyer, M. R. (2001) Stellar Masses in Encyclopedia of Astronomy and Astrophysics. Nature Publishing Group & Institute of Physics Publishing. Hampshire, U.K.

McAlister, H. (1977) Speckle Interferometric Measurements of Binary Stars. I. The Astrophysical Journal 215, [159-165].

McAlister, H., & Hendry, E.M. (1982) Speckle Interferometric Measurements of Binary Stars. VI. ApJS 48, [273].

McAlister, H. (1988) Seeing Stars with Speckle Interferometry. American Scientist. Vol. 76:2, [166-173].

McAlister, H. (1992) Encyclopedia of Physical Science and Technology. Academic Press, San Diego. Vol. 15, [668].

Michelson, A.A. (1891) Measurement of Jupiter's Satellites by Interference.

Nature 45, [106-161].

Monnier, J.D. (2003) Optical Interferometry in Astronomy. Reports on Progress in Physics Volume 66 No. 5, [789-857].

Muller, P. (1984) Measurements of binary stars performed at Nice (Second series). Astronomy and Astrophysics Supplement Series. Vol. 57, [467-486].

Orlov, V.G., Voitsekhovich, V.V., Mendoza-Valencia, G.A., Svyryd, A., Rivera, J.L., Ortiz-Trejo, F. & Guerrero, C.A. (2009) RevMexA&A 45, [155].

Perryman, M. (2012) Astronomical Applications of Astrometry: Ten Years of Exploitation of the Hipparcos Satellite Data. Cambridge University Press, Cambridge.

Pavlovic, R. & Todorovic, N. (2005) Serbian AJ 170, [73-78].

Prieur, J.-L., Scardia, M., Pansecchi, L., Argyle, R.W., & Sala, M. (2012) MNRAS 422, [1057].

Raghavan, D., McAlister, H.A., Henry, T.J., Latham, D.W., Marcy, G.W., Mason, B.D., Gies, D.R., White, R.J., & Brummelaar, T.A. (2010) A Survey of Stellar Families: Multiplicity of Solar-Type Stars. The Astrophysical Journal Supplement Series, 190, [1-42].

Reid, I.N., & Gizis, J.E. (1997) Low-Mass Binaries and the Stellar Luminosity Function. Astronomical Journal, 113, [2246-2269].

Rowe, D. & Genet, R. (2014) User's Guide to PS3 Speckle Interferometry Reduction. In preparation.

Scardia, M. (2001) Inf. Circ. 144.

Scardia, M. (2003) Inf. Circ. 149.

Siegler, N., Close, L.M., Cruz, K.L., Martín, E.L., Reid, I.N. (2005) Discovery of Two Very Low Mass Binaries: Final Results of an Adaptive Optics Survey of Nearby M6.0-M7.5 Stars. The Astrophysical Journal, 621, [1023-1032].

Shara, M., Doxsey, R., Wells, E.N., and McAlister, H. (1987) The fraction of close binaries among Hubble Space Telescope guide stars – operational consequences, workarounds, and suggestions for designers of future space observatories. *Publ. Astron. Soc. Pacific* 99, [223-233].

Teiche, A.S., Genet, R.M, Rowe, D., Hovey, K.C., Gardner, K.C. (2014) Automated Speckle Interferometry of Double Stars. Journal of Double Star Observations. Vol. 10 No. 4.

Tokovinin, A. (1985) Interferometric Observations of Double Stars in 1983 and 1984.

Astronomy and Astrophysics Supplement Series, vol. 61, [483-486].

Tokovinin A.A., & Ismailov, R.M. (1988) Interferometric observations of double stars in 1985 and 1986. Astron. Astrophys., Suppl. Ser., 72, [563-565].

Tokovinin, A., Mason, B., & Hartkopf, W. (2010) AJ 139, [743].
USNO (2015a) The Washington Double Star Catalog. http://www.usno.navy.mil/USNO/astrometry/optical-IR-prod/wds/WDS.

USNO (2015b) Neglected Doubles. http://ad.usno.navy.mil/wds/wdstext.html#neglected.

USNO (2015c) The Sixth Catalog of Orbits of Visual Binary Stars. http://www.usno.navy.mil/USNO/astrometry/optical-IR-prod/wds/orb6.

van Leeuwen, F. (2007) Validation of the new Hipparcos reduction. Astronomy and Astrophysics. Volume 474, Issue 2, [653-664].

Worley, C.E. & Heintz, W.D. (1983) Pub. U.S. Naval Obs. 24, pt. 7.

Zirm, H. (2008) Inf. Circ. 166.